Experimental Thermal and Fluid Science 163 (2025) 111408

Contents lists available at ScienceDirect

Experimental Thermal and Fluid Science

journal homepage: www.elsevier.com/locate/etfs

Exploring exudate absorption via sessile droplet dynamics in porous wound dressings

Avick Sinha [a,b], Anastasios Georgoulas [a,b,*], Cyril Crua [c], Shirin Saberianpour [a,d], Dipak Sarker [a,d], Rachel Forss [a,e], Matteo Santin [a,d]

[a] Centre for Regenerative Medicine and Devices, Brighton, BN2 4GJ, Sussex, UK
[b] Advanced Engineering Centre, University of Brighton, Brighton, BN2 4GJ, Sussex, UK
[c] School of Engineering and Informatics, University of Sussex, Brighton, BN1 9QJ, Sussex, UK
[d] School of Applied Sciences, University of Brighton, Brighton, BN2 4GJ, Sussex, UK
[e] School of Education, Sport and Health, University of Brighton, Brighton, BN2 4GJ, Sussex, UK

ARTICLE INFO

Keywords:
Droplet
Wound dressing
Porous material
Simulated body fluid
Wound exudate

ABSTRACT

Chronic wounds, typically defined as those that fail to reduce in size by at least 40% within a month, present a significant global socioeconomic challenge. In clinical practice, it is widely recognized that maintaining an optimal moisture balance in the wound while managing excess exudate is crucial for wound healing. Therefore, the selection of wound dressings is a key tool in wound management, which is based on their ability to sustain this delicate equilibrium. However, there is a notable lack of fundamental studies on the interaction between wound exudate and dressings, which limits the availability of evidence-based guidance for clinical practitioners. Thus, the present investigation explores how wound exudate interacts with different commercially available wound dressings to optimize wound management through a deep understanding of exudate-air interface dynamics in contact with the dressing material. Employing high-resolution imaging, the research delves into the behaviour of quasi-sessile droplets on various porous materials, analysing the impacts of exudate viscosity, blood sugar levels, and exudate volume. The findings reveal that droplet absorption rates depend on exudate properties and dressing materials. Notably, cellulose-based dressings outperform alginate and polyester-based alternatives in terms of wettability and imbibition capacity, with a performance improvement of at least 48%. Furthermore, increased exudate viscosity and elevated blood sugar are associated with longer absorption times, with increases of ≈ 51% and ≈ 38%, respectively. The study also identifies that absorption completion time increases exponentially with fibre diameter but decreases with greater pore radius and higher porosity. The overall findings can aid clinicians with quantitative insights to optimize the selection of wound dressings, thereby enhancing the healing of chronic wounds.

1. Introduction

Chronic or difficult-to-heal wounds are typically defined as those that have not reduced by more than 40% to 50% in size or healed within one month after injury [1,2]. Treating chronic wounds is a significant concern in the healthcare system due to the delayed healing process and high financial burden. The global prevalence of chronic wounds is projected to be 1.51 to 2.21 per 1000 individuals [3], and the incidence is anticipated to increase with aging populations worldwide [4]. In the United States (US), it is estimated that 2 to 4.5 million people are affected by chronic wounds, costing the US economy around $25 billion per year [5]. Thus, chronic wounds impose tremendous physical, emotional, and financial consequences on individuals and society [6], necessitating further research to promote efficient wound healing.

Wound exudate plays a significant role in the wound healing process. It is a plasma-like material that supplies critical nutrients and molecules for healing. The volume and viscosity of wound exudate vary based on its size, nature, and location [7]. However, there are few established instruments for practitioners to quantify exudate accurately, and descriptions often rely on clinician experience [8]. Melotto et al. [9] demonstrated that animal exudate samples classified within the same category (seropurulent) can exhibit varying viscosities depending on their composition. This variability in viscosity will significantly affects absorption rates, nutrient diffusion, and microbial

* Corresponding author at: Advanced Engineering Centre, University of Brighton, Brighton, BN2 4GJ, Sussex, UK.
E-mail address: A.Georgoulas@brighton.ac.uk (A. Georgoulas).

https://doi.org/10.1016/j.expthermflusci.2025.111408
Received 5 November 2024; Received in revised form 11 December 2024; Accepted 5 January 2025
Available online 11 January 2025

growth—factors that directly influence wound healing. Thus, a clinician's experience for wound assessment may not always be adequate, emphasizing the need for more precise, data-driven evaluation methods.

Wound dressings have long been employed to manage wound exudate and promote healing. Various biomaterials, both hydrophobic and hydrophilic, are used to support wound healing. Synthetic polymers and natural biopolymers like methylcellulose (for moderate to high exudate wounds) and alginate (for bleeding wounds) are applied throughout treatment until the wound closes [10]. Clinicians aim to minimize disruption to the wound bed by using a layered approach: a primary dressing made of a hydrophobic polymer with limited swelling properties, followed by a more hydrophilic secondary dressing with higher swelling capacity. This method maintains a moist environment while controlling exudate. In the final healing stages, dressings with limited swelling properties are typically used [10]. Thus, a knowledge of the dressing material composition is vital to understand the exudate-dressing interface characteristics as it is expected that exudates will penetrates more easily in case hydrophilic porous material as compared to the hydrophobic materials.

With over 3000 dressing options on the market, clinicians face challenges in managing all aspects of wound care and the nature of wound dressings [11]. In-vivo clinical trials are the most effective way to evaluate wound dressings. However, too few have been conducted and published [12,13]. Existing research has investigated how wound dressing materials interact with cells involved in the healing process of acute surgical wounds. In a study of six cases by Shirin et al. [14], it was found that when Atrauman dressing retained healing-related cells (such as endoglin-expressing cells and M2 macrophages) at the wound site, the healing process progressed smoothly. However, in cases where Melolin dressing absorbed these key cells into its mesh, healing was slower or even worsened. This is due to the distinct material compositions and physicochemical properties of the two dressing. However, these findings does not highlight anything about the physics behind interaction of the exudate with the biomaterials and regarding the absoprtion of the exudate. Forss [15] explored the relationship between exudate viscosity and absorption rates in wound dressings, demonstrating that both the fluid's viscosity and the type of dressing play critical roles in absorption dynamics. Forss observed that higher viscosity fluids take longer to be absorbed, particularly when interacting with low-absorbent dressings and it was suggested the need for tailored dressing selection for effective wound management. However, Forss study did consider several factors such as dressing pore size and fibre size, material composition, and the interplay of these characteristics, which can significantly influence absorption efficiency. In a recent review paper by Nguyen et al. [16], it was noted that while modern wound dressings have evolved to tackle clinical challenges, their effectiveness still heavily depends on their interaction with diverse exudate properties, such as viscosity and glucose levels—an area that remains insufficiently understood. This limitation reduces the real-world applicability of many wound dressings. By incorporating the analysis of various exudate properties into wound dressing absorption dynamics, this study aims to bridge the gap between laboratory testing and clinical application, ensuring that dressings are better suited to meet the complex demands of chronic wound care.

Porous wound dressings can be involved in various actions, including absorption, gelling, retention, and moisture vapour movement. Irrespective of the mode of action, it is imperative to understand that their interaction with the exudate may alter the overall wound/dressing interface. If a dressing fails to absorb high-viscosity exudate, it can cause the wound to deteriorate rather than heal. Most research on wound dressings focuses primarily on keeping the wound moist and preventing infection [15]. This indicates that more studies are needed to evaluate these wound dressing products quantitatively and conduct clinical trials to help clinicians choose the proper wound dressings. Thus, as a first step, quasi-sessile/sessile droplet experiments need to be conducted to understand the underlying physics behind the interaction of exudate with various commercially available wound dressings.

A plethora of studies have been carried out on drop impacts on solid surfaces and liquid layers [17], and moving liquid films [18]. However, limited literature focuses on droplet impact on a complex porous topology such as wound dressings, involving spreading, penetration, or both. The authors are unaware of any previous experimental or numerical studies on the impact of a quasi-sessile droplet on commercially available wound dressings. The present study is of direct interest in better wound management by understanding the complex physics behind the exudate-dressing interaction. This investigation not only sheds light on interface dynamics but also provides high-fidelity validation data for Computational Fluid Dynamics-based multiphase models. These numerical models can be used for testing several factors that are not practically feasible to measure during the experiments. This work is also applicable in various engineering domains, such as understanding the absorption of raindrops in soil [17], spraying of fuel droplets onto the porous coating of the piston crown to increase vapourisation [19], and inkjet printing [20]. A few related works on liquid droplet absorption into porous materials are summarized below.

Wallace and Yoshida [21] conducted one of the earliest experiments on drop impact on permeable surfaces, primarily investigating the spread factor, which is the ratio of the maximum diameter of the liquid in contact with the surface after it flattens on the surface to the initial diameter of the droplet before it touches the surface, concerning impact energy for pesticide spray application. Building on Wallace and Yoshida's initial exploration of spreading factors, Startov et al. [22] used CCD cameras and monochromatic lights to investigate the spreading of a droplet on various porous surfaces with different working fluids. They divided the spreading process into two stages. In the first stage, the droplet spreads on the surface with the imbibition front expanding marginally ahead of the spreading droplet. In the second stage, the droplet spread radius decreases until it completely disappears, while the imbibition front continues to expand until the droplet is fully absorbed. They observed that the dynamics of droplet spreading and imbibition vary depending on drop size and viscosity.

Delbos et al. [23] conducted a preliminary study on droplet imbibition inside a porous surface, considering a single pore. They observed that at low impact velocity (< 1 m/s) and smaller pore sizes, a hydrophobic pore prevents permeation, while a hydrophilic pore allows the droplet to be sucked in. At higher impact velocities and larger pore diameters, a portion of the drop penetrates inside the capillary pore, forming a slug inside the capillary tube. Bouchard et al. [24] further investigated the penetration of water and ethanol droplets into a single capillary. They observed that for all Weber numbers, ethanol droplets cleave more readily than water droplets due to lower surface tension.

Sahu et al. [25] conducted experimental and numerical investigations to study liquid droplet impact on a horizontal fibre. They found that increasing the ratio of droplet diameter to fibre diameter reduces the threshold velocity required for a droplet to penetrate hydrophilic fibres. They also noted that droplet penetration is possible when the capillary pressure exceeds the dynamic pressure and that hydrodynamic focusing occurs when the pore diameter is significantly smaller than the droplet diameter. Boscariol et al. [26] also observed that increasing the ratio of dynamic pressure to capillary pressure improves droplet penetration through a mesh-type surface. They further observed that hydrodynamic focusing also plays a role when the droplet diameter exceeds the pore diameter.

Lee et al. [27] investigated droplet impact and spreading on natural porous stones and found that the porous stones did not absorb liquid due to inertial effects after impact. Instead, the liquid was absorbed by capillary action, which began after the droplet reached its maximum spread. They also observed that an air layer between the droplet and porous substrate causes dynamic non-wetting behaviour, resulting in a hydrophobic contact angle greater than 90°. These findings connect to the work of Startov et al. on spreading dynamics and the observations

of Delbos et al. on capillary action. Ryu et al. [28] carried out further studies on how the wettability of water drops affects hydrophobic and superhydrophobic meshes. They found that hydrophobic surfaces require a higher impact velocity for penetration, but super-hydrophobic meshes can allow penetration at lower speeds. They hypothesized that the difference was caused by hydrodynamic focusing and momentum transfer from the drop when it bounced from the surface.

Lipson and Chandra [29] examined droplet impact on porous stainless steel and observed that the droplet impact results in a thin film drawn into pores by capillary forces. They noted that the rate of droplet spread decreases with greater surface roughness and that droplet spreading increases with a reduction in surface tension. Goede et al. [30] carried out further investigation on the effect of surface roughness of a porous fabric geometry. They found that fabric geometry and roughness significantly influence droplet spreading and increased roughness leads to lower spreading radii due to increased viscous dissipation. They also observed that at low impact velocities (< 1 m/s), there is no significant difference in droplet spread between smooth surfaces and textiles with a substrate. Zhang et al. [31] used high-speed imaging to study droplet impact dynamics on fabrics with different pore diameters. They identified two penetration regimes: partial and complete. In the partial regime, a portion of the droplet passes through the substrate and then most of the droplet volume retracts to the upper surface, while in the complete regime, the droplet expands beyond the textile, forming liquid filaments that shatter into secondary droplets.

Numerical simulations can complement experimental investigations by providing detailed information on velocity and pressure profiles and quantifying fluid volumetric flow rates into pores. Reis et al. [32] developed a computational model using the finite volume approach to investigate the dynamics of a liquid droplet on porous media. They found that lower permeability of the porous substrate increases drag, thereby, reducing liquid penetration and increasing lateral spreading outside the substrate.

Navaz et al. [33] studied the spreading of a sessile droplet on a porous substrate using a continuum approach for liquid and gas phases to investigate the impact of chemical warfare agents with porous media. They observed that the spread of droplets is driven by momentum due to capillary pressure/saturation gradients. In a similar study, Choi et al. [34] observed that the droplet penetration depth inside a porous surface increases with increasing porosity and droplet size. A simplified analog of a quasi-sessile droplet being absorbed by a single cylindrical pore was numerically investigated by Andredaki et al. [7] to evaluate the impacts of pore size, liquid viscosity, and initial droplet diameter. They found that the initial droplet diameter does not significantly influence liquid absorption characteristics, with pore diameter and liquid properties governing the flow regime inside a single capillary. Basit et al. [35] also observed that viscosity plays a dominant role compared to porosity and impact velocity in reducing the contact angle, while optimal residual drop volume is primarily determined by porosity.

Most past experimental investigations did not consider very small velocities or quasi-sessile droplets. As noted in previous studies, the initial momentum of the droplet significantly impacts liquid penetration and spreading characteristics. Moreover, the impact of porous media on drop spreading remains unclear due to the simultaneous presence of spreading and absorption behaviours and the lack of understanding of contact line behaviour on rough surfaces [34]. Limited numerical studies have investigated the simultaneous spreading and penetration of a sessile droplet on a single pore. However, a single pore structure does not accurately capture the complexity of droplet dynamics on and inside wound dressings. Additionally, the material properties of wound dressings, both physical and chemical, have not been thoroughly considered, despite their significant effect on droplet absorption characteristics. Thus, the primary objective of the present investigation is to explore the dynamics of quasi-sessile droplet interaction with various wound dressings using high spatial–temporal resolution imaging. Viscosity, blood sugar level, and exudate volume are critical variables which has a direct influence on the wound healing process and wound dressing interaction [15]. Viscosity influences the flow behaviour of wound exudate, affecting its ability to penetrate dressing pores and determining absorption efficiency. Elevated blood sugar levels, often associated with diabetes, can hinder wound healing by altering the physicochemical properties of exudate, leading to longer absorption times. Exudate volume plays a pivotal role in the dressing's ability to sustain a moist environment essential for healing while mitigating risks like pooling and maceration. A thorough understanding of these factors will offer clinicians valuable quantitative data to optimize dressing selection, bridging a crucial gap in evidence-based wound care practices. Hence, further investigation was conducted to understand the effects of fluid properties including viscosity, blood sugar level, and exudate volume on the absorption efficacy of wound dressings.

Table 1
Wound dressing samples used in the present study.

Material/No.	1.	2.	3.
Polyester	Melolin	Atrauman	Kerramax
Cellulose	Aquacel	Kerracel	NA Ultra
Alginate	Kaltostat		

Table 2
Clinical use of the wound dressings considered in the present study.

No.	Sample	Clinical use
1.	Melolin	Lightly to moderately exuding wounds
2.	Atrauman	Primary dressing
3.	Kerramax	Moderate to heavy exudate wounds
4.	Aquacel	Heavy exudate wounds
5.	Kerracel	Moderate to heavy exudate wounds
6.	NA Ultra	Primary dressing
7.	Kaltostat	Stop Bleeding

2. Experimental: Materials and methods

2.1. Materials

The target samples considered in the present study are seven commercially available wound dressings, which are categorized into three groups based on their material type (polyester, cellulose, and alginate-based wound dressing) as shown in Table 1. Their primary uses are provided in Table 2. These seven samples were chosen because they belong to three distinct groups and analysing them will provide insights into how different material types affect exudate absorption. Thus, it is important to know the dressing material composition as understanding the chemical makeup of wound dressings will provide insights into their physical properties, such as absorbency, flexibility, and adherence, which directly influence their performance in wound management.

Though Melolin (manufactured by Smith & Nephew; https://www.smith-nephew.com/en-gb), Atrauman (manufactured by Hartmann Group; https://www.hartmann.info/en-au/products/) and Kerramax (manufactured by Crawford Healthcare; https://www.foundryhealthcare.co.uk/) belong to the same category, Kerramax typically has a multi-layered design, where different layers serve different purposes. The outer layer of Kerramax is made of polyethene terephthalate fibres that provide strength, durability, and non-stick properties, while the inner layers typically contains carboxymethylcellulose (CMC) fibres, which are highly hydrophilic and absorbent in nature with good moisture retention capability. Atrauman wound dressings are made of a special polyester tulle, while Melolin wound dressings are typically composed of a layer of viscose and polyester fibres. These materials provide a soft and absorbent surface for wound exudate.

For cellulose-based dressings, Aquacel (manufactured by ConvaTec; https://www.convatec.com/en-gb/) dressing is predominantly composed of sodium carboxymethylcellulose (NaCMC) fibres, which are

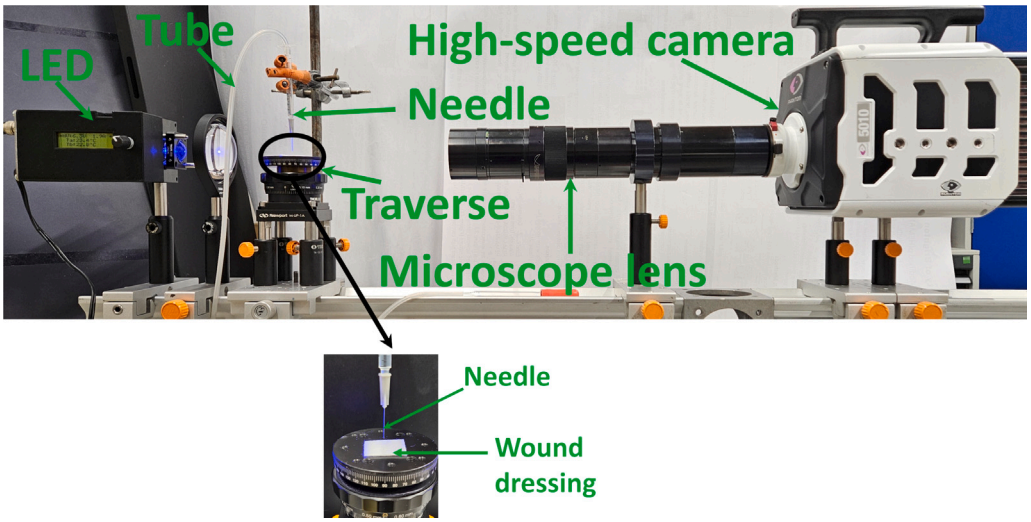

Fig. 1. Experimental test rig setup with a high-speed camera, microscopic lens, LED lighting and syringe.

water-soluble and form a gel-like matrix upon exposure to wound exudate. In contrast, Kerracel (manufactured by Crawford Healthcare) dressings are made entirely of carboxymethylcellulose (CMC) fibres, renowned for their exceptional hydrophilicity and absorbency. These fibres also transform into a gel-like matrix when in contact with exudate, promoting moisture retention and facilitating wound healing.

The NA Ultra wound dressing (manufactured by 3M; https://www.3~m.com/3M/en_US) features a proprietary blend of materials, including hydrocolloids, non-adhesives, absorbent fibres, and moisture-retaining polymers, carefully tailored to each product variant. As NA Ultra dressing is non-adhesive, it typically requires the use of secondary dressings, adhesive tapes, or bandages to hold it in place over the wound.

Lastly, Kaltostat (manufactured by ConvaTec) comprises predominantly of calcium sodium alginate fibres sourced from seaweed, which undergo gelation upon contact with wound exudate. This unique feature endows Kaltostat dressings with exceptional absorbency, as the calcium sodium alginate fibres transform into a gel-like matrix upon exposure to exudate. For a more detailed description of the material composition of the wound dressings mentioned, please refer to the respective manufacturer websites linked above.

2.2. Solutions

Simulated Body Fluid (SBF) were used as a biologically-safe surrogate for wound exudate to investigate the interaction between the dressing and the bodily fluid (including exudate) during the wound healing process. SBF mimics the ionic composition of human plasma, hence, making it a suitable surrogate for in-vivo conditions [36]. The simulated body fluid was prepared as per the technique suggested by Pietrzyńska and Voelkel [37].

As wound exudates can be of various viscosities depending on the nature, location, and size of the wound, it is essential to investigate the effect of viscosity on wound dressing absorption. To examine the impact of viscosity on wound dressing absorption, Dextran Blue (DB) with a molecular weight of 2×10^3 kg/mol (Sigma-Aldrich) was introduced into the simulated body fluid (SBF) at a concentration of 2 mg of DB per ml of SBF, effectively increasing the solution's viscosity to approximately 1.26 times that of pure SBF. Dextran molecules, being long-chain polysaccharides, can create entangled networks within water, impeding the solution's flow and consequently elevating its viscosity. It is important to note that the incorporation of Dextran Blue into SBF does not involve any specific chemical reaction; instead, it entails the dissolution and dispersion of dye molecules throughout the solution. The solution takes on a blue hue due to the presence and dispersion of Dextran Blue dye molecules.

Table 3
Viscosity and surface tension of the working fluids at 20 °C.

No.	Fluid	Dynamic Viscosity (μ, mPas)	Surface tension (σ, mN/m)
1.	SBF	0.968 ± 0.018	70.73 ± 1.59
2.	SBF+Glucose	0.977 ± 0.014	68.19 ± 1.81
3.	SBF+DB	1.222 ± 0.024	68.77 ± 2.14

In hyperglycemia conditions, wound exudate may contain higher levels of glucose ($C_6H_{12}O_6$) compared to normal conditions. This can impair the body's ability to heal wounds effectively, prolonging the healing process and potentially leading to complications such as delayed wound closure and increased risk of infection [38]. Foot problems with diabetes are widespread and costly, and diabetics account for over half of all hospital admissions for amputations. In the United Kingdom, diabetics account for more than 40% of major amputation hospitalizations [39]. Thus, it is important to investigate how the presence of glucose in exudates will affect the rate of absorption in wound dressings. In the present study, we have considered 11 mmol/L (critical value for hyperglycemia condition [38]) of glucose per ml of SBF.

The physical properties of the working fluids used in the present study are shown in Table 3. From Table 3, it is evident that the addition of DB to SBF increases its viscosity by 26%. Additionally, a slight decrease in surface tension values was observed with the addition of both glucose and DB compared to pure SBF. It is important to highlight that although adding glucose to SBF does not significantly alter the solution's viscosity, a marked increase in droplet absorption time in the wound dressing was observed when glucose is added to SBF as shown later in Fig. 12.

2.3. Experimenal set-up

The experimental test rig configuration is shown in Fig. 1. The optical set-up included an LED lighting source (manufacturer: Cree; XB-D) which was utilized to provide continuous illumination and a high-speed camera (manufacturer: Phantom; TMX 5010) coupled with a long-distance microscopic lens (manufacturer: Infinity Photo-Optical Company; K2). The camera and the LED light were aligned along the same axis to maintain uniform lighting and minimize potential shadow and glare.

The exposure period was set at 5 μs to capture the images. Images were captured with a high temporal resolution of 20 kHz and a

spatial resolution of 1024 × 1024 pixels to observe the microsecond-scale phenomenon of drop imbibition. Following calibration, the spatial sensitivity of the long-distance microscope was determined to be 10 μm/pixel.

Droplets were generated by propelling air through a small syringe connected to a larger syringe using a pneumatic tube. This air propulsion creates a droplet at the tip of the utilized hypodermic needle, which subsequently detaches and descends toward the wound dressing under the force of gravity. Two different needle sizes (27G and 23G) were considered in the study to investigate the effect of exudate volume on wound dressing absorption characteristics. The nominal inner diameter of the 27G needle is 0.21 mm, and the average droplet diameter (D_D) generated from this needle across all cases is 2.13 mm ± 0.07 mm (95% confidence interval). For the 23G needle, with a nominal inner diameter of 0.34 mm, the mean droplet size generated across all cases is 2.58 mm ± 0.05 mm (95% confidence interval). The reason for using a larger droplet diameter compared to the fibre diameter is to prevent rapid absorption of the droplet into the wound dressings. To minimize the kinetic energy of the droplet, the release height was kept as minimal as possible. The droplet impact velocity (V_0) was calculated by measuring the distance it covered in several successive frames before contacting the dressing and was found to be 0.025 ± 0.001 m/s. The Weber number ($We = \frac{\rho V_0^2 D_D}{\sigma}$), calculated using the larger droplet diameter and properties of the simulated body fluid (SBF), is 0.023, where ρ is the fluid density (≈ 998.2 kg/m^3). This value of We remains relatively consistent across different fluids since the variations in surface tension between SBF and other fluids are not substantial. The Ohnesorge number ($Oh = \frac{\mu}{\sqrt{\rho\sigma D_D}}$) based on the larger drop diameter is 0.002 and 0.003 for the SBF and SBF + DB case, respectively. Such small values of We, and Oh numbers suggest that surface tension forces predominantly influence the droplet behaviour during impact. Another significant dimensionless number is the capillary number, $Ca = \frac{\mu V_0}{\sigma}$, which quantifies the relative significance of viscous forces compared to surface tension forces at the liquid-gas interface. For the various solutions tested, Ca is on the order of 10^{-4}, further confirming that the viscous forces are relatively small compared to surface tension forces.

The Bond number ($Bo = \frac{\Delta\rho g(D_D/2)^2}{\sigma}$) quantifies the relative importance of gravitational forces compared to surface tension forces. For the largest droplet diameter, Bo is ≈ 0.95. In this context, g represents the acceleration due to gravity, and $\Delta\rho$ is the density difference between the droplet and the surrounding medium. Since Bo < 1, this indicates that surface tension forces are more significant than gravitational forces, meaning the droplet is expected to maintain a nearly spherical shape during impact.

2.4. Image processing

All acquired images underwent comprehensive analysis in MATLAB to explore the dynamics of the considered droplet-wound dressing interactions. The number of images analysed depended on the droplet absorption time, ranging from a minimum of 500 to a maximum of 30,000 (with each experiment repeated at least three times to ensure reliability and accuracy of results). An illustration of the image processing algorithm is shown in Fig. 2. Enhancements in contrast and sharpness were applied to the images, ensuring that the physical features depicted in the images were more readily recognizable and distinguishable. The images were then cropped to decrease computational time by removing unwanted areas of the image. Following this, the images were binarised and the *hfill* function was used to fill the holes in the droplets. After this, the edges around the droplet were calculated and then considering the longest edge and vertical height, the edges of the droplet were separated into left and right edges (marked in red and blue colour under the heading Separating edges in Fig. 2). Finally, based on the elliptical fit, the contact angle between the tangent of the ellipse and the contact line was obtained for both the left and right-hand sides of the droplet

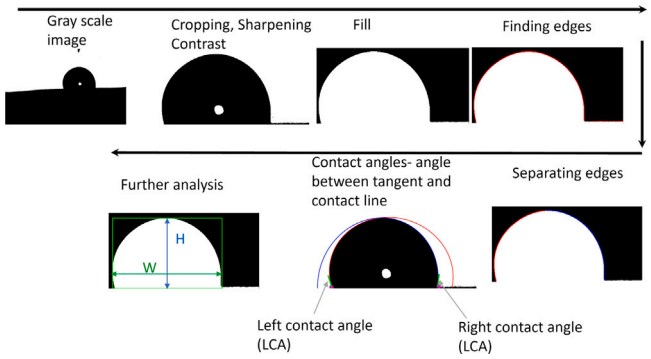

Fig. 2. Algorithm for droplet characteristics analysis.

to determine the left (LCA) and the right (RCA) contact angles. The dynamic apparent contact angle (θ_d) is calculated based on the mean of the LCA and RCA together. Further analysis of the droplet spread diameter (W) and height (H) was also carried out to obtain the volume of the droplet above the dressing surface.

3. Results and discussion

3.1. Wound dressings structural characteristics

Obtaining the three-dimensional structure of wound dressings is crucial for assessing their topology, fibre diameter, and porosity, all of which are vital for understanding their performance in wound management. The two-dimensional structure of the dressing samples was characterized by confocal microscopy (ZEISS LSM 800). The microscope captured an area of 638.9 μm ×638.9 μm with a spatial resolution of 0.62 μm/pixel. By stacking several two-dimensional images through the vertical plane, the three-dimensional structure of the wound dressings was reconstructed (shown in Fig. 3).

From the images, it is evident that although Atrauman and NA Ultra have different chemical compositions, they share a similar knitted fabric sheet structure. Similarly, both Kerramax and Kaltostat exhibit an open structure, whereas Kerracel and Aquacel dressings feature a non-woven fabric or mesh-like arrangement. Melolin, on the other hand, displays densely woven zig-zag fabric patterns, contributing to its layered structure. This detailed characterization provides valuable insights into the design and performance variations among different wound dressings.

From Table 2, it can be noted that both Atrauman and NA Ultra are used as primary dressings meaning these dressings are always in direct contact with the wound, unlike the other dressings which can be used as secondary as well. Additionally, both Atrauman and NA Ultra have a knitted structure. Thus, from a clinical viewpoint, Atrauman and NA Ultra are grouped under “knitted”, while Aquacel, Kerracel, and Kaltostat are grouped under “natural-based” polymers since both cellulose and alginate fibres are naturally derived. There is no change in the group for Melolin and Kerramax; they remain under the “polyester-based” dressings. This grouping has been consistently followed throughout this study.

An in-house MATLAB code was employed to analyse fibre diameter and porosity from the 500 2-D stacked images, with the mean fibre diameter depicted in Fig. 4(a). The stacked images are segmented to distinguish fibres from voids, using thresholding techniques that separate pixel intensity levels corresponding to solid structures (fibres) and empty spaces (pores). To measure fibre diameter, cross-sectional regions of the fibres are identified, and their dimensions are calculated, by fitting circles to the segmented regions. The average diameter is determined across the entire dataset. For porosity, the ratio of void space to the total volume of the material is computed by summing the pixel

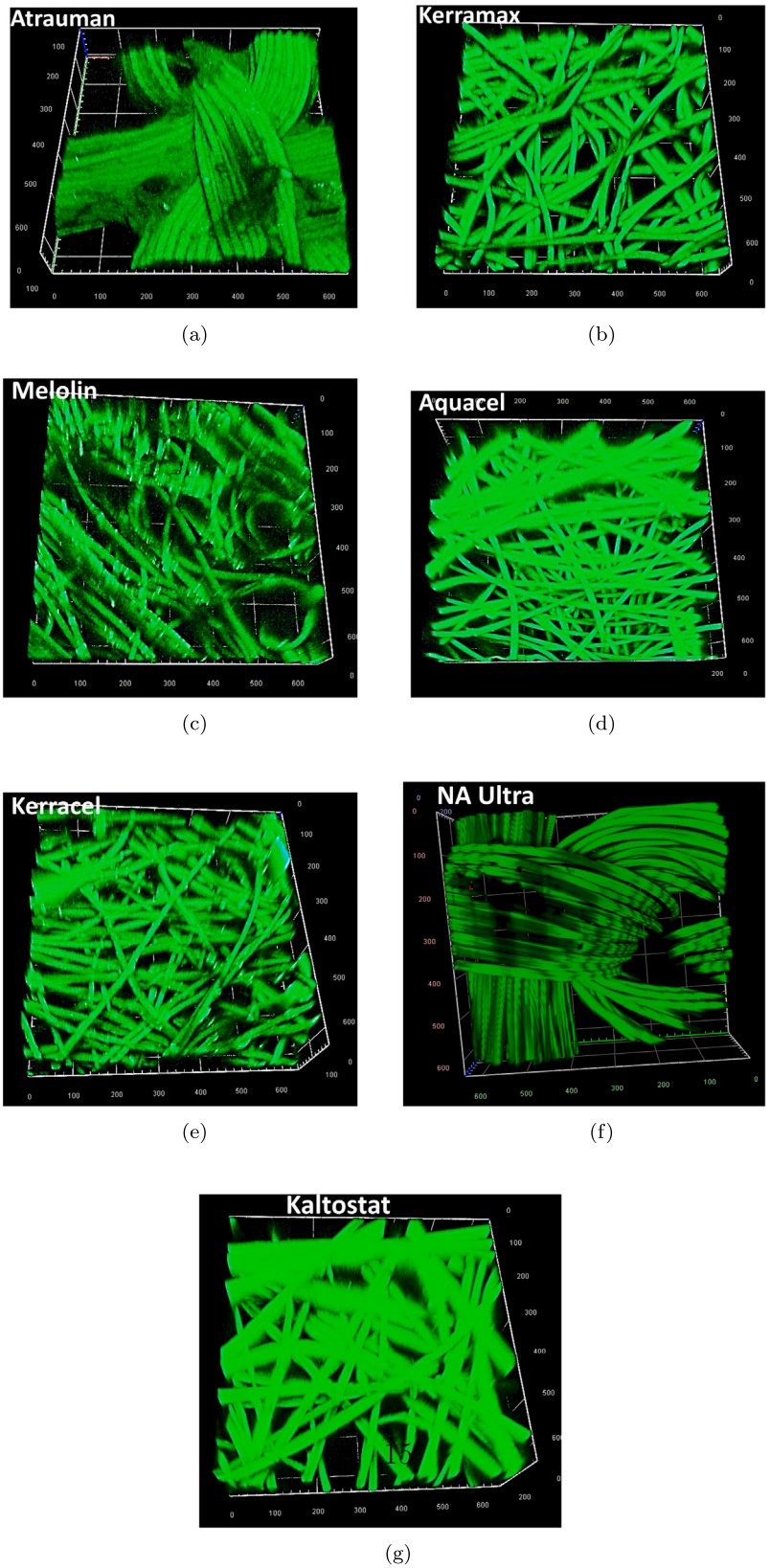

Fig. 3. 3-D confocal images of the considered Wound dressing (a) Atrauman (b) Kerramax (c) Melolin (d) Aquacel (AQ) (e) Kerracel (f) NA Ultra (g) Kaltostat.

intensities of void regions and dividing by the total number of pixels in the image stack. Similarly, pore diameter is calculated by identifying the boundaries of void spaces and measuring their maximum inscribed circle diameters. This process is repeated across all images, and the average pore diameter is obtained. The porosity and pore diameter (D_p) is calculated based on the algorithm used by Rabbani et al. [40].

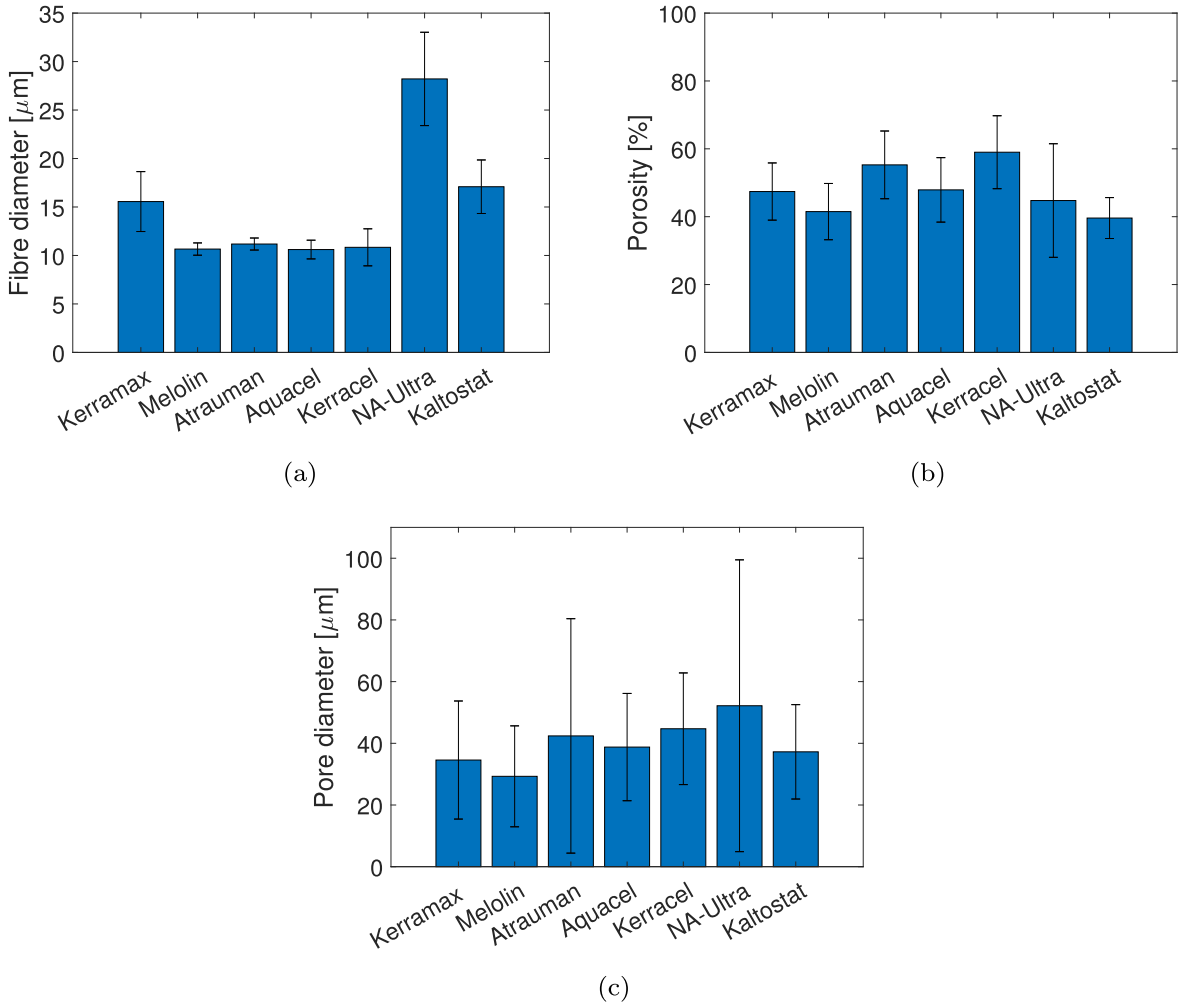

Fig. 4. Dry Fibre (a) Diameter (b) Porosity (c) Pore diameter.

NA Ultra displays the largest fibre diameter, followed by Kaltostat and Kerramax. Larger fibre diameters in wound dressings may enhance absorption capacity by providing greater surface area for fluid interaction, potentially allowing for increased absorption of wound exudate or fluids. Conversely, the fibre diameter of other wound dressings exhibits minimal variation within the uncertainty limit. The porosity of each wound dressing is illustrated in Fig. 4(b). Kerracel demonstrates the highest porosity followed by Atrauman, Kerramax and Melolin. Higher porosity in wound dressings facilitates greater fluid absorption and retention, promoting wound healing and maintaining a moist wound environment. Though porosity provides a general indication of the void space within a material, pore radius offers additional information about the size distribution of these voids, which is important to better comprehend the material's structure and behaviour. From Fig. 4(c), it can be observed that the pore diameter is maximum for NA Ultra followed by Kerracel and then Atrauman. Both NA Ultra and Atrauman are knitted structures, indicating the large parallel space between the two fibres. The uncertainty in NA Ultra and Atrauman wound dressings is also quite high because of the small gaps between the two knitted layers along with the large spaces. Thus, the uncertainty bars reveal the diversity of pore sizes within an individual wound dressing. Despite the high uncertainty, the mean value offers a baseline for understanding the distribution of pore sizes. Furthermore, it can be observed that Kerracel has a larger pore diameter as compared to Aquacel and Kaltostat. For the polyester-based dressings, Kerramax exhibits a larger pore diameter compared to Melolin, indicating greater fluid permeability for the former dressing.

The structural characteristics of the wound dressings, as estimated, can be effectively linked to their clinical applications, as summarized in Table 2. Melolin, with moderate fibre diameter and small pore size, reduces absorption speed, making it ideal for lightly exuding wounds where excessive fluid uptake is unnecessary [41] Atrauman, characterized by a knitted polyester structure with large porosity and moderate fibre diameter, exhibits slower absorption due to its hydrophobic nature, making it suitable as a primary layer to protect the wound bed and prevent adherence to wound tissue [42]. Kerramax, with moderate porosity and fibre diameter combined with a multi-layered construction, enhances fluid handling, making it effective for absorbing moderate to heavy exudate and preventing maceration in chronic or infected wounds [43]. Aquacel, with moderate porosity and hydrophilic properties, is optimal for heavy exudate wounds, providing moisture retention and bacterial barrier capabilities [44]. Kerracel, featuring high porosity and pore diameter with carboxymethylcellulose (CMC) fibres, absorbs fluid efficiently while maintaining a moist wound environment, making it particularly suitable for chronic or surgical wounds with moderate to heavy exudate [45] NA Ultra, with its knitted structure, high porosity, and large pore and fibre diameters, excels at absorbing fluid while minimizing adherence, making it suitable as a primary dressing or under compression bandages for wounds with light to moderate exudate [46]. Lastly, Kaltostat, composed of alginate fibres with moderate fibre diameter and porosity, supports moderate fluid

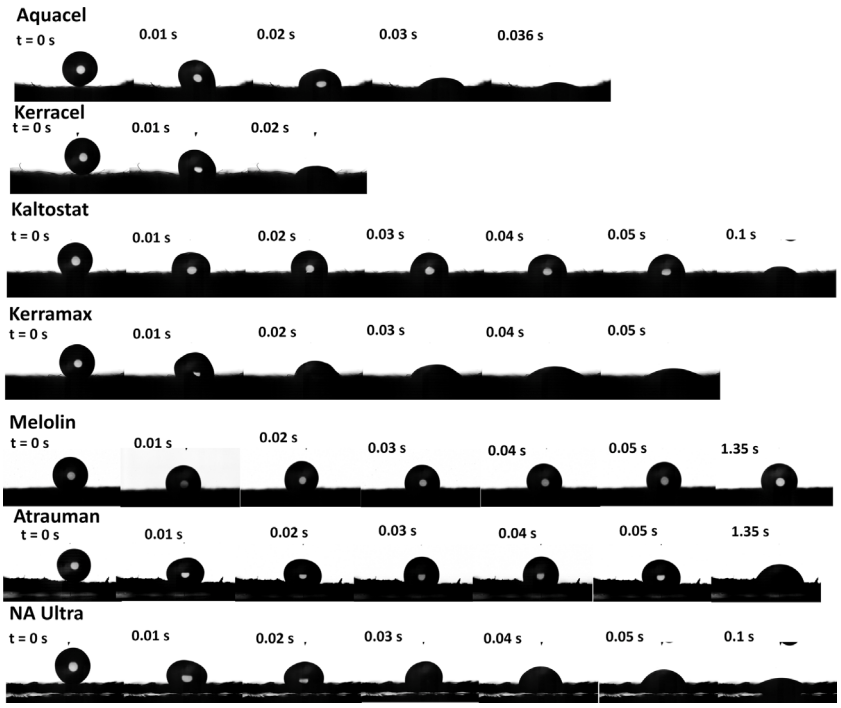

Fig. 5. Temporal evolution of the droplet shape on the various wound dressing. The working fluid is SBF and D_D is 2.13 mm.

absorption and is ideal for bleeding wounds due to its hemostatic properties and moderate exudate management capabilities [47]. For heavy exudate wounds, dressings with high porosity and moderate pore sizes (e.g., Kerracel, Aquacel) are recommended, while for light exudate, lower porosity and hydrophobic surfaces (e.g., Atrauman, Melolin) are more appropriate. Larger pores will facilitate faster imbibition for high-viscosity fluids, whereas smaller pores will maintain prolonged contact for lower-viscosity exudates.

It is important to note that measuring the surface roughness of wound dressings is challenging due to their complex, irregular structures and non-uniform surfaces. This inherent variability complicates the use of standard techniques, making it difficult to obtain consistent and representative roughness measurements, hence, not measured in the present study. However, it is assumed that the surface roughness is of the same order as the fibre diameter.

3.2. Qualitative analysis of the droplet dynamics

Fig. 5 illustrates the time evolution of the droplet interacting with the various wound dressings considered, for $D_D = 2.13$ mm and with SBF as the working fluid. Unless stated otherwise, the present study maintains consistency in D_D and SBF as the working fluid. Given the dense concentration of fibres, capturing the flow phenomenon within them posed a challenge. Consequently, the camera could only capture the dynamics of droplets outside the porous substrate. Interestingly, it is observed from Fig. 5, that the droplet shape after landing on any wound dressing is significantly deformed with time as it penetrates/spreads or both. This could be because the capillary forces are stronger at the edges of the droplet, where the curvature is higher, causing the liquid to be drawn preferentially into these regions. Moreover, the size and shape of the pores vary, leading to non-uniform deformation of the droplet as it encounters different regions of the porous medium.

A qualitative analysis of the images reveals two distinct outcomes when a droplet lands on a wound dressing: complete penetration and partial imbibition. Partial imbibition is defined as the state in which most of the droplet volume remains at the top of the porous surface at an equilibrium state, while a small portion of the droplet has penetrated within the porous media. Partial imbibition occurs exclusively with Melolin and Atrauman while complete penetration is observed with other wound dressings. Focusing first on the complete penetration phenomenon, upon droplet landing, the small initial momentum propels the droplet sideways due to the rapid pressure increase at the impact point. At the same time part of the droplet is moving downwards in the vertical direction. This dual action results in a simultaneous spreading and penetration of the droplet along and into the porous medium. Initially, the inertial force of the droplet facilitates spreading, which is countered by surface tension and viscous forces. Eventually, as the spreading slows down, the penetration continues inside the pores due to capillary action.

In this study, it is important to highlight that the dynamic pressure at the point of impact (ρV_0^2) is significantly lower than the capillary pressure ($\frac{4\sigma}{D_p}$), considering that D_p is on the order of 10^{-6} while V_0^2 is on the order of 10^{-4}. As a result, the condition for static penetration, which typically requires $\rho V_0^2 \gg \frac{4\sigma}{D_p}$, is not met in this scenario. Instead, the initial droplet penetration (primarily for Atrauman and Melolin, which are made of hydrophobic fibres) can be attributed to hydrodynamic focusing, as D_p is notably smaller than D_D. This substantial difference between the droplet and pore diameters enhances the liquid's kinetic energy at the pore entrances, resulting in a pore velocity (V_P) $\approx \frac{D_D}{D_p} V_0 \approx 100 V_0$ for liquid entering the pore. Consequently, such high liquid velocity within the pores induces shaped-charge (Munroe) jets [48], which are coherent, well-defined fluid streams ejected from a small orifice under pressure. It is worth noting that comparable high velocities, arising from the accumulation and directed flow of kinetic energy dictated by geometry (small size of pores), have been predicted and observed previously [49,50]. This phenomenon also resembles the high-speed jets observed near the bottom region of incompressible droplet impacts on liquid layers [49]. Thus, it can concluded that the penetration of droplets into the wound dressing material is due to the combined action of both hydrodynamic focusing and capillary forces. Hydrodynamic focusing helps to direct the fluid flow into the pores of the dressing, while capillary forces drive the liquid deeper into the porous structure, ensuring efficient and rapid absorption of exudate.

The viscous effect will be relatively unimportant near the pore entrance as the pore Reynolds number (Re_P) for the working fluids

considered is $O(10^2)$ based on $D_P \approx 50$ μm and $V_P \approx 2.5$ m/s. To investigate the viscous dissipation effect of an exudate flowing through the wound dressing, the viscous shear stress (τ) needs to be determined, which can be estimated as [25]:

$$\tau \approx \frac{\mu V_0 D_D}{D_P^2}$$

The surface area of droplet-dressing interaction is influenced by both the pore size and droplet diameter. Therefore, when a droplet engages with a pore, the contact area can be approximated by factoring in the dimensions of both components. The simplest approximation for this interaction area is a rectangle with dimensions D_D and D_p. Thus, the surface area of a single pore will be of the order of $D_D D_p$ ($D_P \approx 50$ μm, $D_D \approx 2.58$ mm and $V_P \approx 2.5$ m/s), then the viscous friction force (F_V) on a single pore is $\approx \tau D_P D_D$. If the exudate enters into the dressing through several pores in the order of $(\frac{D_D}{D_p})^3$, the total viscous force will be in $O(F_V(\frac{D_D}{D_p})^3)$. If the exudate has wetted a thickness of h_p inside the dressing, the total viscous dissipation will be $\approx \tau\ D_D D_p\ (\frac{D_D}{D_p})^3\ h_p \approx O(10^{-1})$. This indicates negligible viscous dissipation inside the wound dressing pores. Thus, most of the energy dissipation inside the pore is due to surface tension. A similar form of total viscous dissipation was also used by Sahu et al. [25] for a hydrodynamic focusing penetration of fluid into a porous medium.

Considering a flow velocity inside the pore of around 2.5 m/s (based on V_0= 0.025 m/s), and assuming the thickness of the top few layers of the wound dressings to be ≈ 2 mm across all cases, the time required to fill this space is on the order of 10^{-3} s. In contrast, the time for complete droplet spreading over the wound dressing is on the order of 10^{-2} s, indicating that pore filling is virtually instantaneous against the backdrop of droplet spreading. As dynamic wettability is impacted by pore geometry, it can lead to diverse rates of liquid absorption among different wound dressings of the same type for an equivalent volume of liquid.

In natural wound dressings, the time required for Aquacel and Kerracel to reach complete imbibition is significantly different as exhibited in Fig. 5. By 0.03 s, the droplet on Aquacel has maintained a small portion above the dressing, whereas on Kerracel a complete penetration has occurred. This difference can be attributed to the higher porosity and pore diameter of Kerracel compared to Aquacel. This complete imbibition phenomenon for both Aquacel and Kerracel, make them effective in managing wounds with moderate to heavy exudate, particularly chronic wounds or surgical sites that require consistent moisture levels. Comparing Kaltostat (alginate-based dressing) with Aquacel and Kerracel (cellulose-based dressings), it is evident that the droplet in the case of Kaltostat exhibits slower penetration rates due to the lower porosity and pore diameter of the dressing. Additionally, cellulose-based fibres exhibit greater hydrophilicity than alginate-based fibres due to their chemical composition. Cellulose is composed of glucose units linked by $\beta(1 \rightarrow 4)$ glycosidic bonds, which form a polar structure with abundant hydroxyl (-OH) groups present in SBF. These groups engage in strong hydrogen bonding with water molecules, augmenting cellulose's hydrophilic nature. Conversely, alginate, derived from seaweed, comprises a linear copolymer of β-*D*-mannuronic acid and α-*L*-guluronic acid residues. Although alginate also contains hydroxyl groups, they are not able to match the absorbency capacity and speed of cellulose-based dressings, especially in managing heavy exudates [51,52]. The slower penetration in case of Kaltostat (compared to cellulose-based dressings), makes it suitable for bleeding wounds requiring hemostasis and moderate exudate management.

Comparing, two polyester-based dressings: Kerramax and Melolin, it can be observed from Fig. 5 that in the case of Melolin there is a partial imbibition and after the maximum spreading, the droplet is pinned on the surface due to its hydrophobic nature, indicating that the cohesive forces within the droplet are stronger than the adhesive forces, preventing complete penetration. This behaviour makes Melolin suitable for lightly exuding wounds. Its controlled absorption will prevents over-drying of the wound bed, and its hydrophobic nature minimizes excessive fluid retention, which is unnecessary in low-exudate cases. However, for Kerramax, after the reduction in the maximum width due to surface tension, complete imbibition occurs, which could be attributed to its higher porosity and pore diameter as compared to Melolin. Moreover, Kerramax wound dressing includes a combination of CMC and superabsorbent polymers which contributes to its ability to absorb and retain fluid as compared to Melolin which contains a polyester mesh coated with a soft, perforated film of low-adherent polyethylene, leading to significantly slower penetration and incomplete absorption [53,54]. This enables Kerramax to efficiently manage moderate to heavy exudate in chronic or infected wounds, reducing the risk of maceration and promoting a healthy wound environment.

Lastly, comparing the two knitted wound dressings (Atrauman and NA Ultra), it can be observed that complete penetration occurs in NA Ultra, while in Atrauman partial imbibition occurs. The difference in the droplet dynamics is due to the different chemical compositions of these wound dressings, while NA Ultra is composed of cellulose, Atrauman is a polyester-based wound dressing. A complete penetration in the case of NA Ultra makes it suitable as a primary dressing for wounds with light to moderate exudate. For Atrauman, it is observed that when the droplet comes into contact with the wound dressing, a certain amount of fluid penetrates. The liquid fills the void spaces within the dressing primarily due to hydrodynamic focusing. However, as the droplet penetrates the porous medium, surface tension forces act to minimize the surface area of the droplet causing the droplet to contract and recoil. Eventually, a dynamic equilibrium is reached between the capillary forces driving droplet penetration and the surface tension forces, causing the droplet to stop recoiling. At this equilibrium point, the droplet remains stable within the porous medium, with the forces of penetration and recoil balanced. This partial imbibition makes Atrauman suitable as a primary dressing for protecting the wound bed, particularly when adherence to tissue must be avoided and for wounds with minimal exudate, providing a barrier while preventing maceration.

The qualitative assessment of the images provides a visual insight into the dynamic behaviour of droplets, which in turn aids in identifying the different regimes. However, these observations alone are limited in providing conclusive insights, necessitating integration with quantitative analysis. The droplet eccentricity results in Section 3.3 further enrich this understanding by quantifying the droplet shape dynamics during absorption. Kerracel exhibited a sharp increase in eccentricity, reflecting rapid penetration and spreading, while Melolin maintained a stable, lower eccentricity, aligning with its partial imbibition behaviour. The dynamic contact angle measurements in Section 3.4 corroborate the qualitative findings by quantifying the wettability of the dressings. Melolin and Atrauman displayed stable, high contact angles, confirming their lower wettability and limited absorption capability. In contrast, Kerracel and Aquacel showed rapid reductions in contact angle, consistent with their hydrophilic nature and efficient fluid uptake as observed in Section 3.2. Finally, the imbibition analysis in Section 3.5 quantified the absorption percentages, providing definitive evidence of material performance. Kerracel, Aquacel, Kaltostat and NA Ultra shows complete imbibition within short time frames, validating their high absorption capacity seen in qualitative observations. Details on the various quantitative analysis are provided in the below sections. This detail quantitative analysis will aid in the optimization of dressing selection for enhancing patient comfort.

3.3. Droplet eccentricity

Droplet eccentricity is a crucial parameter in evaluating the interaction of the working liquid with the considered wound dressings. In the context of droplet shape analysis on surfaces, eccentricity is a measure of the deviation of the droplet's shape from a perfect circle (a sphere from a three-dimensional viewpoint). An eccentricity of 0 means the

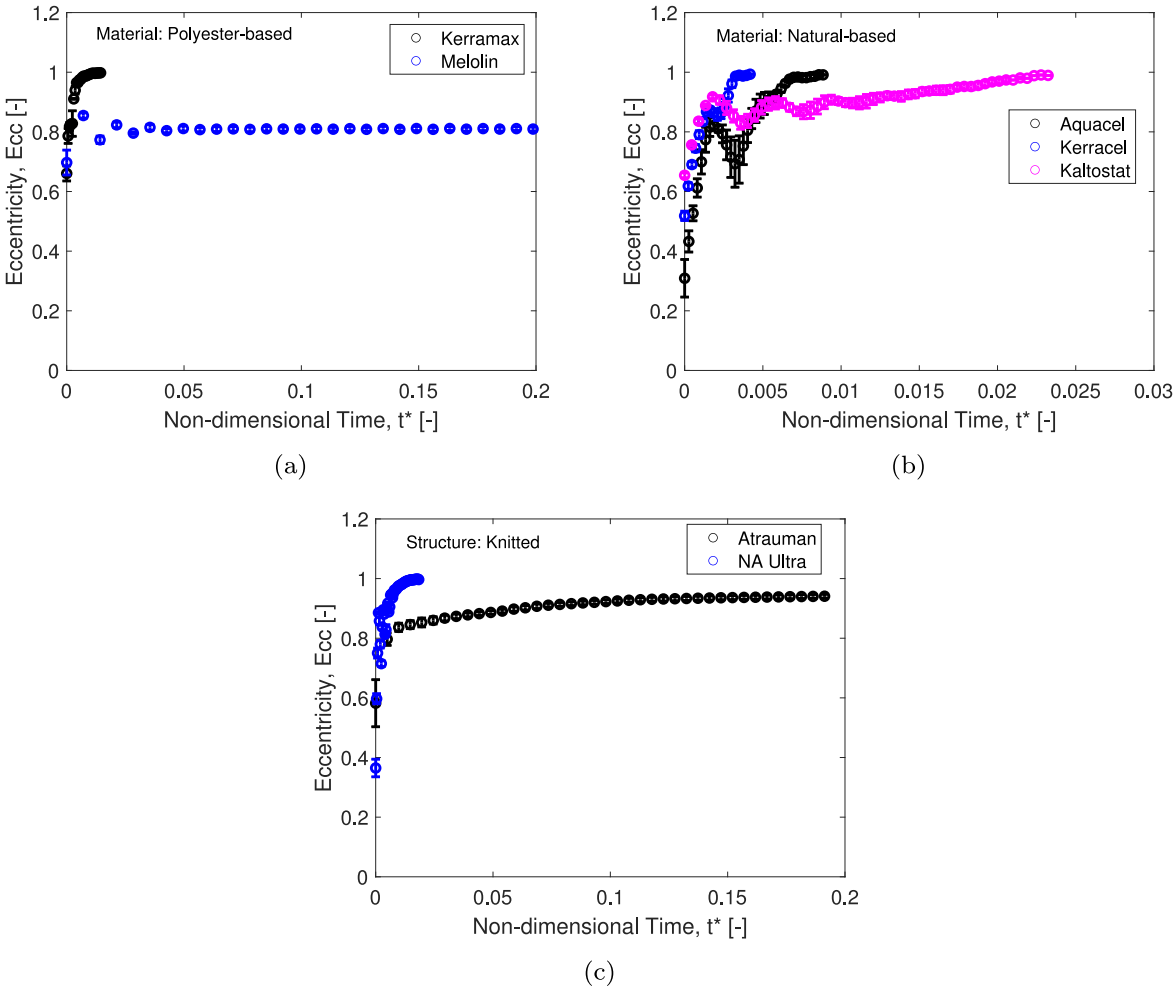

Fig. 6. Droplet eccentricity against non-dimensional time, $t^* = \frac{t\mu V_0^2}{2r_p\sigma}$: Comparison of various dressing material types—(a) Polyester and (b) Cellulose. Comparison of the same structural type—(c) Knitted.

droplet's shape is a perfect circle. When a droplet is perfectly circular, this indicates that the forces acting upon it are symmetrical, and it is not being distorted by external influences. In contrast, an eccentricity of 1 would indicate that the droplet's shape is a straight line, which is an extreme and theoretical case for droplets on a surface. In practical terms, an eccentricity closer to 1 (but less than 1) means that the droplet is very elongated or oval-shaped. This could happen because almost all of the volume of the droplet has already penetrated inside the substrate. A low eccentricity suggests that the working liquid is held nicely in place and maintains a good shape for optimal wound coverage, while a higher eccentricity may indicate more spread or almost no liquid left on the substrate or the droplet is asymmetrical/tilted.

Fig. 6 shows the droplet eccentricity against non-dimensional time (t^*) for various wound dressing groups. In this study, dimensional time (t) is normalized using $\frac{t\mu V_0^2}{D_p\sigma}$. This normalization form is chosen as it incorporates liquid properties and pore radius (D_p), which are crucial parameters governing droplet characteristics in porous media. Using the Buckingham Pi theorem, other non-dimensional forms of time were derived, such as $\frac{\mu D_p t}{\sigma}$, $\frac{tV_0^2}{D_p}$, and $\frac{tV_0}{\mu\sigma}$. However, none of these forms succeeded in collapsing the curves for eccentricity, dynamic contact angles or droplet imbibition. As this non-dimensional time form $\frac{t\mu V_0^2}{D_p\sigma}$ represents the scenario as observed during the experiments, hence, it is utilized in this study.

It is important to emphasize that while Fig. 6 presents the droplet eccentricity for all the dressings, the comparison within the same material types is specifically highlighted in Fig. 6(a) and Fig. 6(b), for polyester-based and natural-based materials, respectively. In contrast, Fig. 6(c), compares dressings with similar structural types. The dressings are presented together in a single figure to make it easier for readers to compare and analyse the data. To ensure consistency, the plots for surface wettability (Fig. 7) and imbibition (Fig. 9) are presented in a similar format unless specified otherwise.

Fig. 6(a) shows the droplet eccentricity for two polyester wound dressings: Kerramax and Melolin. Qualitatively, it can be observed that Kerramax exhibits a quick increase to a high eccentricity, indicating rapid deformation of the droplet upon impact, followed by a plateau, suggesting a steady state. In the case of Kerramax, a complete penetration of the droplet occurs. Melolin shows a less dramatic change in eccentricity, implying a different interaction between the droplet and the dressing surface. For the case of natural-based wound dressings, the droplet in Kaltostat maintains a higher eccentricity for a longer time compared to the droplets in the other two dressings (Aquacel and Kerracel), suggesting that Kaltostat is able to retain the shape of the droplet without a quick spreading. In contrast, the droplet in Kerracel shows a sharp increase in eccentricity early on, followed by a gradual decrease, which might indicate quick spreading and then stabilization. The droplet in Aquacel results in a middle ground between these behaviours. The rapid change in droplet eccentricity indicates spreading or retracting on the surface along with imbibition inside the surface. In all three cases of natural wound dressings, a complete penetration of the droplet occurs.

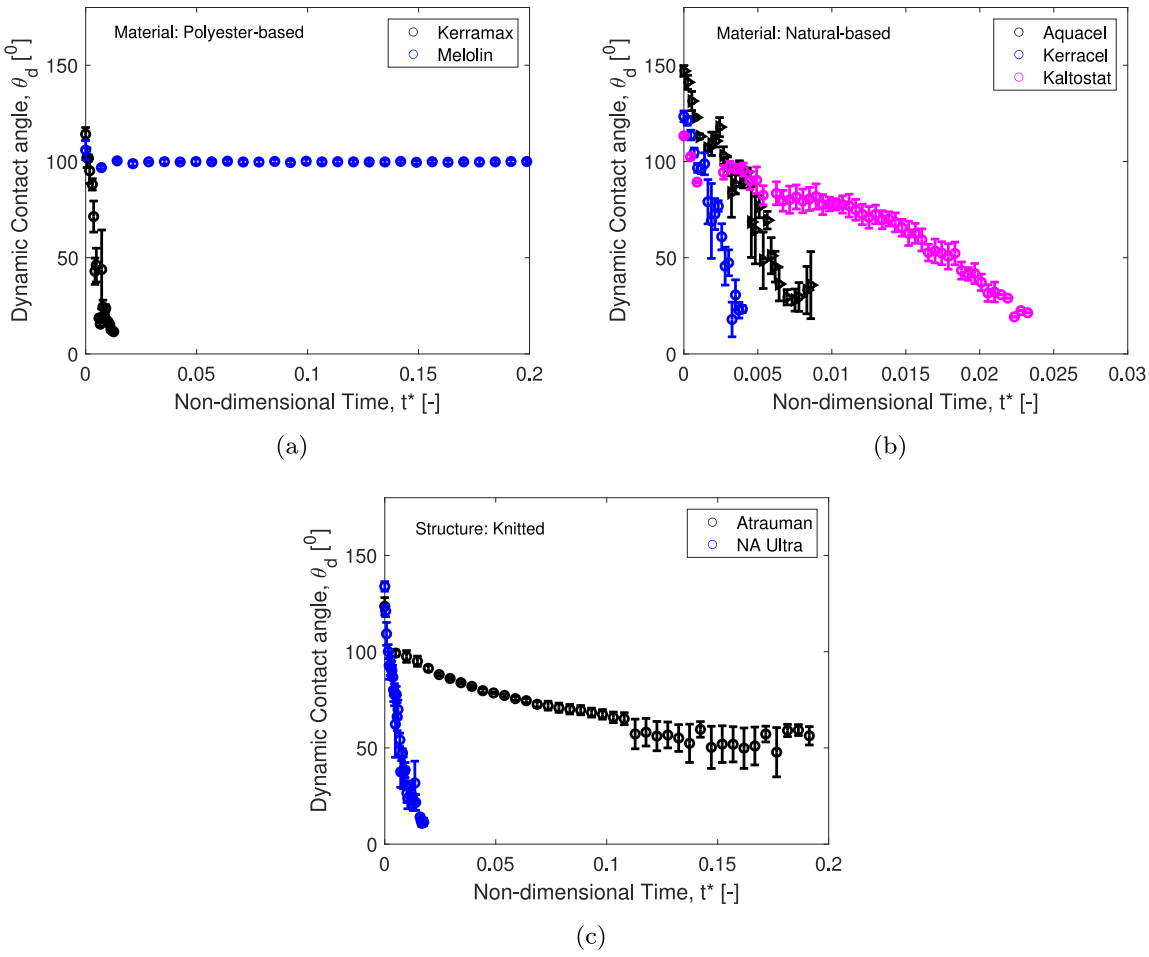

Fig. 7. Dynamic contact angle (θ_d) versus non-dimensional time: Comparison of various dressing material types—(a) Polyester and (b) Cellulose. Comparison of the same structural type—(c) Knitted.

Lastly, qualitatively comparing the two knitted structures, Atrauman and NA Ultra, the droplet in the latter exhibits a quick increase to a high eccentricity, while the droplet eccentricity in Atrauman remains almost constant with the increase in time, indicating that the droplet is pinned on the substrate and at equilibrium.

The results from Fig. 6 can also be linked with the clinical applications in Table 2. A rapid increase of eccentricity to 1 observed in Aquacel and Kerracel indicates rapid penetration and absorption, making them ideal for moderate to heavy exudate wounds requiring high fluid uptake and gel formation. Melolin and Atrauman show a constant eccentricity, reflecting slower absorption and droplet stability, which suits light exudate wounds needing controlled fluid management. Kaltostat's moderate rate of increase to eccentricity to 1 supports balanced absorption dynamics, aligning with its role in bleeding wounds for hemostasis and moderate exudate management, while NA Ultra's rapid eccentricity increase highlights its effectiveness in managing light-to-moderate exudate with non-adherence properties.

It should be noted that though the t^* values for Melolin and Atrauman exceed 1, however, displaying the complete range of t^* will obscure the clarity of the corresponding curves. Therefore, the t^* values for Melolin and Atrauman have been predominantly limited to 0.2 in this study.

3.4. Surface wettability

Fig. 7 shows the dynamic contact angle (θ_d) of the considered wound dressings over time. The dynamic contact angle is an indicator of the hydrophilicity of the dressing material. When the contact angle is below 90°, the meniscus formed in a dressing capillary is expected to be concave within the empty pore space. This results in negative capillary pressure, creating a pressure gradient that encourages wetting of the porous medium. Conversely, a contact angle exceeding 90°, leads to a convex meniscus and positive capillary pressure. Here, the capillary pressure resists liquid propagation into the porous medium, requiring the liquid to overcome this resistance for penetration. Lower angles suggest that the dressing is more hydrophilic and thus may be more effective at managing wound exudate. Each wound dressing demonstrated a distinct dynamic contact angle behaviour, which is reflective of their material composition and structure affecting their liquid handling properties.

Fig. 7(a) illustrates that θ_d for Kerramax decreases rapidly from 114° to 11.5° between $t^* = 0$ and $t^* = 0.012$. This rapid decrease in dynamic contact angle concerning surface energy reflects a significant alteration in the Kerramax material interaction with the liquid. The surface energy dictates the affinity of a material's surface to a liquid phase. When the dynamic contact angle rapidly decreases, it implies that the material is undergoing transformations that enhance its ability to interact with the liquid. This transformation could be due to the interaction between the dressing fibre and SBF or due to physical roughening, which can lead to an increase in the surface area, thereby, enhancing the absorption and distribution of exudate throughout the dressing. In contrast, for Melolin, θ_d asymptotically approaches a constant value of 99.8°, suggesting that Melolin is less effective at fluid management. This limitation may restrict its suitability

for highly exuding wounds, making it more suitable for wounds with lower exudate generation.

Comparison of θ_d for natural-based wound dressings is shown in Fig. 7(b). Kerracel shows a rapid decrease in θ_d from 123.4° to 17.9° with the increase in t^* from 0 to 0.0037 (Fig. 7(b)). This decrease suggests that the liquid is spreading and penetrating more readily across the surface, indicating improved interaction between the liquid and the porous substrate. Aquacel also exhibits a similar trend, followed by a plateau, indicating a quick initial wicking ability that stabilizes over time. θ_d for Aquacel decreases by 111° between $t^* = 0$ and 0.008. The θ_d values for Aquacel remained higher than those for Kerracel at all times, suggesting less efficient liquid management. Interestingly, for Aquacel after the initial decrease a sudden increase occurs and followed by another rapid decrease in θ_d. The possible explanation for this behaviour involve surface rearrangement due to the swelling of the fibre, which will reduce the pore diameter leading to temporary resistance to penetration, and slow filling up of the dense dressing pore will lead to an increase in the contact angle value. Subsequently, as the surface adapts to the new conditions, the contact angle decreases as the liquid phase spreads more uniformly across the surface. Although swelling is expected to occur in both Kerracel and Aquacel, the presence of sodium ions in Aquacel, attributed to Na-CMC fibres, enhances its solubility, which enables the polymer to swell more effectively as compared to Kerracel, which contains only CMC. Consequently, there is a higher chance of decreasing pore radius in Aquacel as compared to Kerracel when in contact with exudate.

It is further observed that droplet in the case of Kaltostat exhibited a remarkably different behaviour compared to the droplets in the other two cellulose-based dressings. The contact angle (θ_d) values remained lower initially, followed by a steady decrease over time, eventually surpassing the values of Aquacel and Kerracel. This suggests that Kaltostat may demonstrate faster initial wicking capabilities but potentially poorer long-term fluid management performance from a clinical perspective.

For knitted and primary dressings, the droplet in Atrauman displayed a steep decrease in θ_d, reaching a stable contact angle quickly. This rapid equilibration suggests that Atrauman has a fast response to its interaction with the liquid, which could be beneficial in the initial phases of wound healing when exudate management is critical. NA Ultra exhibited a similar trend to Atrauman but maintained a consistently lower θ_d throughout its period as shown in Fig. 7(c). This implies that NA Ultra might offer superior liquid handling properties compared to Atrauman from a clinical view point, possibly due to better material composition.

From Fig. 7, it can be observed that for most of the wound dressings (except for Melolin and Atrauman), it is not possible to measure the equilibrium contact angle on the substrate due to the immediate spreading of the droplet and capillary uptake by the substrate. The constant value of θ_d with time for Melolin and Atrauman indicates pinning of the droplet on the substrate and the equilibrium contact angle for Melolin is significantly higher ($\approx$ 42°) than of Atrauman, indicating lower wettability for the former.

The dynamic contact angle results also sheds light on the dressing applications. A rapid dynamic contact angle reduction in Aquacel and Kerracel demonstrates high hydrophilicity for effective fluid wicking, essential for heavy exudate wounds. Kaltostat shows moderate reduction, supporting its gel-forming and hemostatic needs, while Melolin and Atrauman maintain a stable contact angle due to their hydrophobicity, ensuring controlled absorption for light exudate wounds. NA Ultra's low contact angle reflects excellent wettability, ideal for light-to-moderate exudate while avoiding adherence.

The capillary pressure (P_c) will govern the flow dynamics when the liquid is inside the porous medium and it primarily depends on the contact angle (θ) between the liquid and the dressing along with the dimension of the pores. In a mathematical form, it can be represented as, $P_c = -\frac{4\sigma\cos\theta}{D_P}$ [32]. From Fig. 7, it can be observed that P_c will be

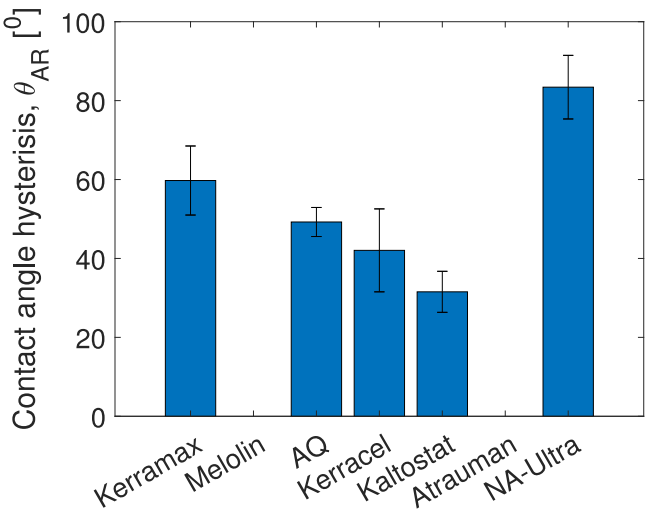

Fig. 8. Contact angle hysteresis for various dressing types.

negative for both Atrauman and Melolin (as the mean magnitude of θ based on the highest and lowest value of θ_d is > 90°,), indicating that the cohesive forces within the liquid are stronger than the adhesive forces between the liquid and the solid and the exudate will be held back from entering the pores. This confirms, that the initial penetration of the fluid inside the pores for Atrauman and Melolin is due to hydrodynamic focussing. For the rest of the wound dressings, the mean value of θ_d is < 90°, indicating the hydrophilic nature of the pores inside the dressing.

It is imperative to investigate the contact angle hysteresis to shed more light on the complex phenomena at the solid–liquid interface and provide insights into the surface characterization by investigating how contact angles change during the spreading and retracting of droplets on the substrate. The contact angle hysteresis (θ_{AR}) was calculated as the difference between the advancing (θ_A) and receding contact angles (θ_R). The advancing contact angle (θ_A) is measured as the droplet starts spreading outwards (advances) on the surface. Once the droplet has reached its maximum spreading, the receding contact angle θ_R is measured when the droplet starts to retract. The differences in the forces at the solid–liquid interface during spreading and retracting are influenced by various factors such as surface roughness, surface chemistry, and surface energy.

Fig. 8 shows that NA Ultra has the highest θ_{AR}, while Kaltostat has the lowest θ_{AR}. A larger hysteresis indicates poor wetting reversibility, i.e., the droplet is less likely to spread or retract easily on the surface. While, low contact angle hysteresis indicates good wetting reversibility, meaning that the droplet will spread and retract smoothly on the surface. For Atrauman and Melolin, θ_{AR} is not calculated as in these dressings the droplet reaches an equilibrium state soon after landing. No significant difference is observed in θ_{AR} for Kerracel and Aquacel, indicating a similar wetting behaviour.

3.5. Imbibition

Fig. 9 shows the imbibition percentage (absorption or uptake of liquid by a material) against a non-dimensional time, t^*. To assess the impregnation characteristics of the wound dressings, the amount of liquid penetration (ϕ_{pen}) is determined by subtracting the volume of the remaining droplet cap (ϕ_{cap}) above the dressing surface from the initial droplet volume (ϕ_0), i.e. $\phi_{pen} = \phi_0 - \phi_{cap}$. The initial droplet volume (ϕ_0) is calculated using the initial droplet radius and assuming the droplet is a perfect sphere, hence, $\phi_0 = (4/3)\pi(D_D/2)^3$. ϕ_{cap} is calculated based on the spread on the spreading diameter (W) and height (H) of the droplet, $\phi_{cap} = \pi H^2(W/2 - H/3)$. Thus, the liquid

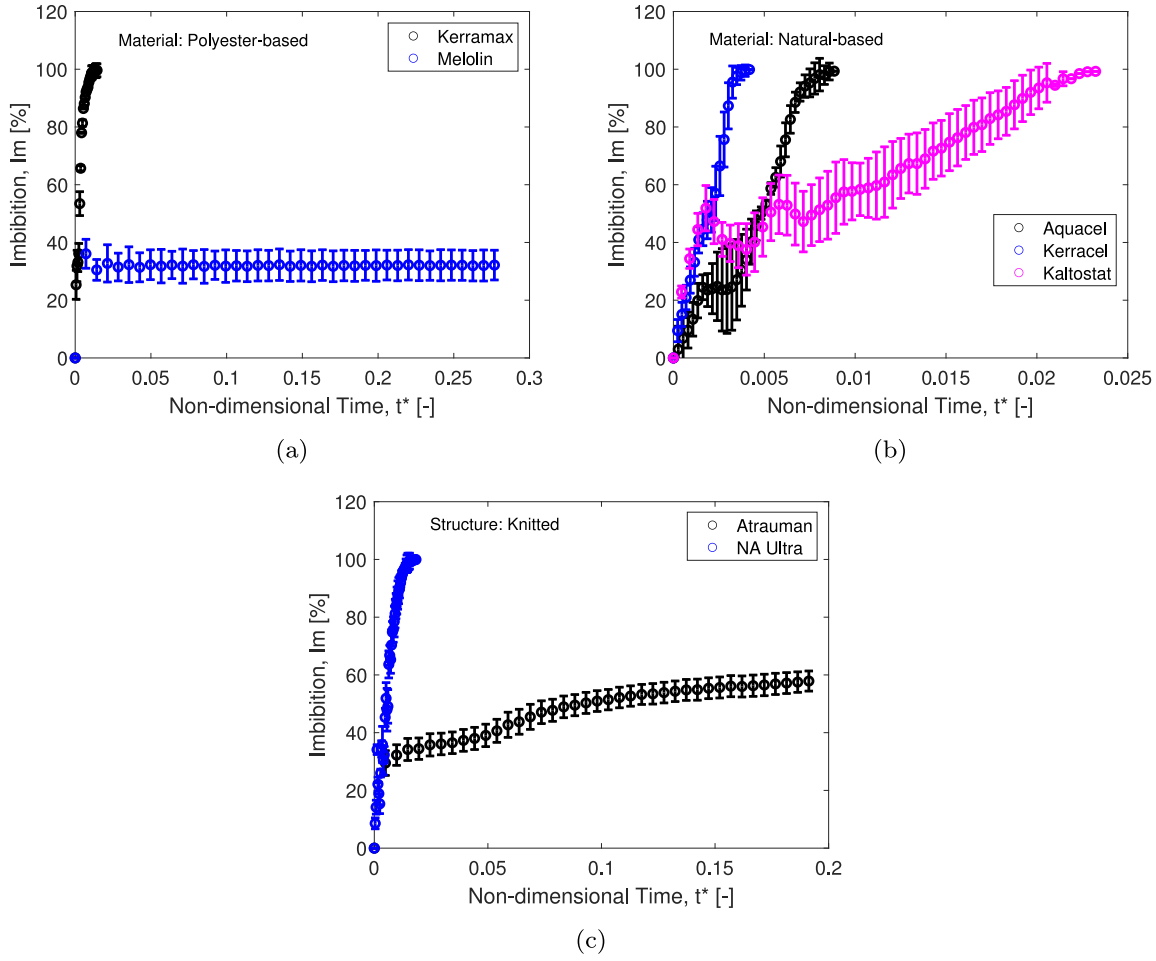

Fig. 9. Imbibition percentage versus non-dimensional time: Comparison of various dressing material types—(a) Polyester and (b) Cellulose. Comparison of the same structural type—(c) Knitted.

penetration can be represented as, $\phi_{pen} = (4/3)\pi(D_D/2)^3 - \pi H^2(W/2 - H/3)$. The same equations were also used by Vontas et al. [55] to calculate liquid penetration below a mesh structure.

For the polyester wound dressings in Fig. 9(a), two very distinct imbibition behaviours are observed. For Kerramax, a steep increase in imbibition to nearly 100% is observed, and the material does not release any liquid after reaching saturation. In stark contrast, Melolin's imbibition is much lower, hovering around 30% throughout the time period. This indicates that Melolin has a much lower capacity for liquid absorption and is highly hydrophobic.

For natural-based dressings, the imbibition curve for Kerracel increases sharply from the beginning and reaches near 100% imbibition relatively quickly. This suggests that Kerracel has a high absorption capacity and is very efficient at taking up liquid in a short period of time. The Aquacel curve also rises sharply but has a more gradual approach to the saturation point compared to Kerracel. This could indicate that Aquacel has a slightly slower absorption rate. In contrast, the Kaltostat curve shows a different pattern, with a slower and more progressive rise in imbibition. The curve does not reach as high a percentage as Aquacel or Kerracel within the same non-dimensional time frame, indicating it may have a slower absorption rate.

Lastly, for the knitted wound dressings, the imbibition percentage for Atrauman increases abruptly, reaching around 50% almost immediately, and then it levels off. This indicates a rapid absorption initially followed by a plateau, where no further liquid is absorbed. This could be useful in applications where a quick uptake of liquid is needed without continuous absorption. The NA Ultra curve is more steeper as compared to Atrauman, indicating faster absorption.

The stabilization of both Atrauman and Melolin curves at a plateau suggests that both materials could be reaching their absorption capacity and that further exposure to exudate will not increase their volume significantly.

From the dressing application view point, the results from Fig. 9 shows that the rapid absorption of Kerracel and Aquacel supports heavy exudate management and moisture retention. Gradual absorption in the case of Kaltostat balances gel formation and fluid management; effective for bleeding wounds. Limited absorption in the case of Atrauman and Melolin will prevents over-drying and maintains light exudate control, while NA Ultra handles light-to-moderate exudate effectively with quick initial absorption.

Studying the ratio of total area to empty area within mesh pores against absorption time is crucial for understanding how wound dressings operate in absorbing exudate. The empty area is the area within the pore boundary. This is crucial for understanding how much additional fluid the dressing can potentially absorb. The total area is the area combined with the pore boundary in addition to the fibre diameter. A schematic diagram showing the fibre diameter, pore diameter and empty area is shown in Fig. 10(a).

This ratio of total to the empty area, denoted as RA, is mathematically defined as $\frac{Area_{Total}}{Area_{Empty}} = \left(1 + \left(\frac{D_F}{D_P}\right)^2\right)$ [55]. Fig. 10(b) illustrates the relationship between these geometric parameters and the non-dimensional absorption time for the SBF cases with a droplet diameter of 2.13 mm (excluding Melolin and Atrauman where droplet

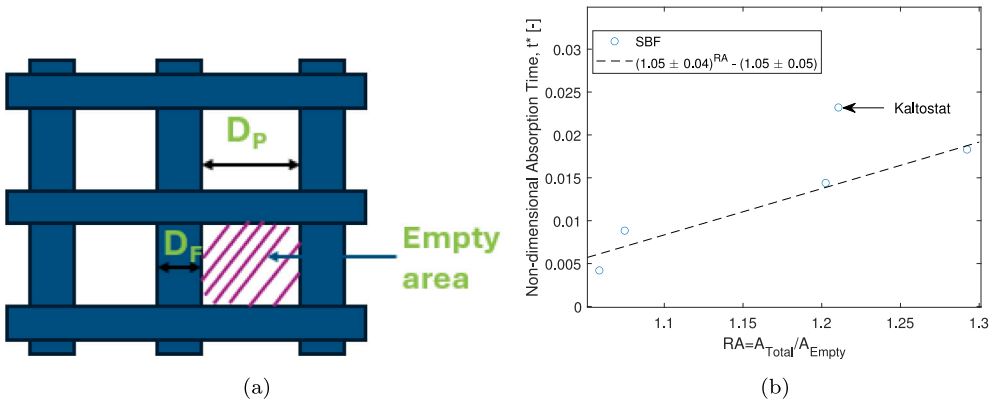

Fig. 10. (a) Schematic diagram showing the empty area, fibre (D_F) and pore (D_P) diameter. (b) Effect of geometrical parameters on the absorption time.

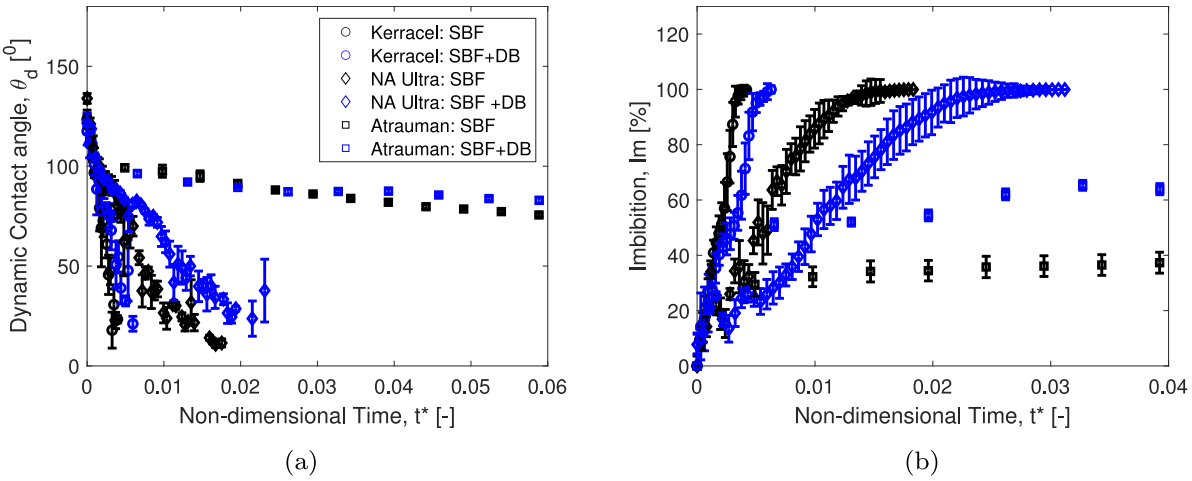

Fig. 11. Effect of increased viscosity on (a) Dynamic contact angle (b) Imbibition. The Dextran Blue fluid is denoted by the blue symbols, while SBF is represented by the black symbols.

penetration was incomplete).

A curve fit based on a 95% confidence level was plotted (indicated by the dotted black line in Fig. 10(b)), revealing an exponential relationship between absorption time and the geometric parameters, except for Kaltostat, which exhibited different behaviour. This indicates that dressings with larger pores or greater porosity can accommodate more exudate, facilitating better fluid penetration and retention. While an increase in fibre diameter correlates with longer absorption times. This knowledge is instrumental in designing wound dressings tailored to optimize absorption capacities, thereby improving wound healing outcomes by maintaining a moist environment conducive to tissue repair.

3.6. Effect of viscosity

A comparison of increased viscosity by adding Dextran Blue to SBF on the θ_d and Imbibition % as compared to pure SBF is shown in Fig. 11. Only three wound dressings were considered for this study: Kerracel, NA Ultra, and Atrauman, as the underlying physics for the other wound dressings with increased viscosity are expected to be similar to those mentioned above.

Fig. 11(a) shows the measure of the dynamic contact angle of three different substrates with and without the addition of Dextran Blue (DB) in simulated body fluid (SBF). The addition of Dextran Blue increases the viscosity of the fluid, resulting in a lower rate of change in the dynamic contact angle because the increased internal friction within the fluid resists rapid deformation and spreading. This resistance can result in a higher initial contact angle and a slower decrease over time as observed in Fig. 11(a). Interestingly, it can be observed that the addition of Dextran Blue to SBF results in a significant change in the dynamic contact angle, particularly noticeable in NA Ultra, which could be due to the smaller number of functional groups in NA Ultra (such as carboxylate groups, COO^-) which are capable of binding or interacting with Dextran Blue.

As expected, the imbibition process is slower when Dextran Blue is added because the fluid's higher resistance to the flow makes it less able to quickly penetrate the porous structure, as depicted in Fig. 11(b). In the case of Kerracel, we do not see a significant difference. This could indicate that the added viscosity helps maintain a more consistent and driven penetration into the material, possibly because of better retention of the fluid within the material's structure. However, for NA Ultra and Atrauman, a significant difference in the absorption time is observed. This is probably because the capillary action, which drives imbibition, is dependent on the balance between cohesive forces within the fluid and adhesive forces between the fluid and the material. Higher viscosity can affect this balance by enhancing the fluid's ability to stay within small capillaries once it has entered them, potentially compensating for the slower movement due to increased fluid resistance.

High-viscosity fluid is well-absorbed by Kerracel, maintaining consistent absorption for chronic or infected wounds. NA Ultra exhibit slower absorption with thick exudates, suitable for wounds requiring retention, while Atrauman remain unaffected due to their hydrophobicity, making them suitable for low-exudate cases.

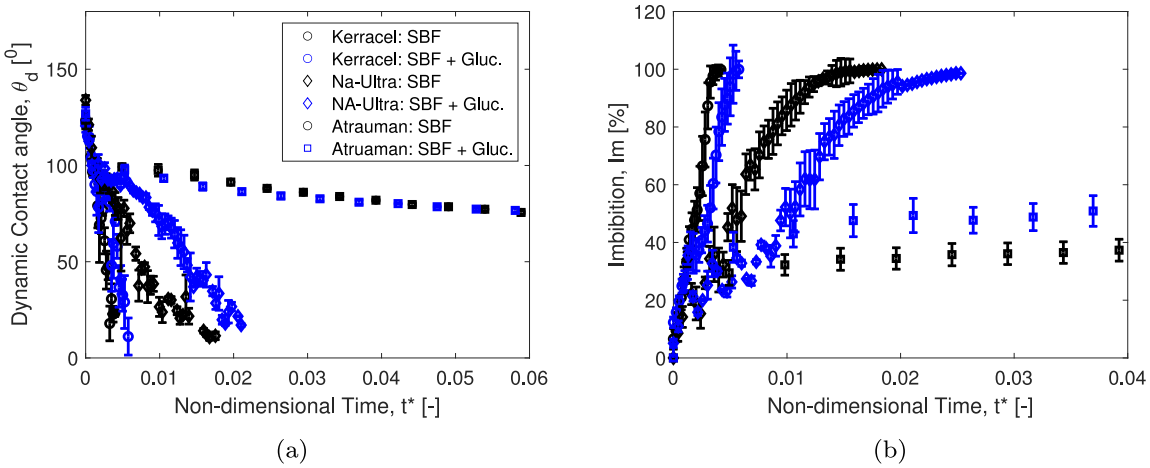

Fig. 12. Effect of glucose level on (a) Dynamic contact angle (b) Imbibition. The hyperglycemia condition is denoted by the blue symbols, while SBF is represented by the black symbols.

3.7. Hyperglycemia condition

A comparison of higher glucose levels in an exudate on the θ_d and Imbibition % as compared to pure SBF is shown in Fig. 12. From Fig. 12(a), it is observed that with the addition of glucose to SBF, the dynamic contact angle for Kerracel and NA Ultra decreases slowly compared to SBF alone, resulting in a reduction in the wettability of the surface. This could be due to several factors such as a reduction in surface tension, an increase in viscosity, or potential chemical interactions with the surface that alter its characteristics. Interestingly, it is observed that the dynamic contact angle in Atrauman does not change significantly with the addition of glucose in SBF, indicating the hydrophobic nature of the surface where the initial spreading behaviour of the fluid remains largely unchanged.

A reduction in surface tension facilitates easier spreading of the liquid across the dressing's surface, enhancing initial wetting but not necessarily accelerating penetration into the material itself. For efficient penetration, the liquid or exudate must navigate through the small pores of the dressing or be drawn by capillary forces, which are enhanced by lower surface tension. This process, while improving absorption capacity, can also slow down overall penetration speed as the substance fills these spaces, resulting in partial saturation within the pores. Therefore, while reduced surface tension enhances initial contact and absorption efficiency, it may paradoxically prolong the time required for complete penetration and saturation of the dressings. Consequently, the wound dressings show a rapid initial increase in imbibition percentage, which slows down over time as shown in Fig. 12(b).

It should also be noted that glucose may also interact with the materials of the wound dressing, potentially forming hydrogen bonds that can modify the dressing's absorption dynamics. These interactions might slow down the movement of fluid through the dressing matrix, further increasing the absorption time.

From application perspective, Kerracel absorb glucose-laden fluids more slowly making them effective for diabetic wounds with heavy exudate. NA Ultra balance slower uptake, suitable for diabetic wounds with moderate exudate, while Atrauman manage low-exudate diabetic wounds with limited interaction.

3.8. Exudate volume

With the increase in the droplet diameter from 2.13 mm to 2.58 mm, the volume of the droplet, and in turn the volume of the exudate, increases by 77.7%. A comparison of the dynamic contact angle and imbibition percentage for two different exudate volumes and two different wound dressings (Kerracel and NA Ultra) is shown in Fig. 13. It is observed from Fig. 13(a) that when the droplet volume increases, the dynamic contact angle does not change significantly for both dressings. This is because the surface tension and viscosity of the liquid resist the deformation of the droplet, maintaining its shape and preventing significant alterations in the contact angle, indicating that the fluid properties govern the wound dressing wettability characteristics.

Interestingly, it is observed from Fig. 13(b) that with the increase in droplet volume, the droplet penetrates a little bit faster for both Kerracel and Aquacel but without any significant increase. This is because larger droplets experience greater gravitational forces, which enhance their penetration inside the dressing. Moreover, when the droplet size increases, it comes in contact with a greater number of pores, reducing the possibility of fluid saturation inside the pores and leading to a faster absorption time.

High exudate volume seems to improves absorption speed for Kerracel making it ideal for heavy-exudate wounds with significant fluid loads, while NA Ultra manage high volumes effectively with rapid initial absorption and gel formation.

3.9. Correlation matrix

From the previous sections, it was observed that the absorption time of exudate primarily depends on viscosity, porosity, and pore radius. In this study, a correlation matrix heat map based on experimental data and MATLAB correlation algorithm was used to visualize relationships between absorption time and these parameters, as illustrated in Fig. 14. The Pearson correlation coefficient is used to quantify the strength and direction of the linear relationship between the various variables (porosity, viscosity, etc.) and absorption time. The correlation coefficient is calculated by dividing the covariance of two variables by the product of their standard deviations. This normalization ensures that the coefficient's value ranges between −1 and 1, providing a standardized measure of the between the variables [56].

In Fig. 14, each cell in the matrix represents the correlation coefficient between two variables. The colour bar indicates the strength of the correlation coefficient, ranging from −1 to +1. A value of 0 in the colour bar indicates no correlation, meaning the variables are independent. A value of +1 indicates a perfect positive correlation, where as one variable increases, the other also increases proportionally, and −1 indicates a perfect negative correlation, where as one variable increases, the other decreases proportionally.

As expected, the correlation between absorption time and itself is 1, reflecting the inherent property of correlation coefficients. The

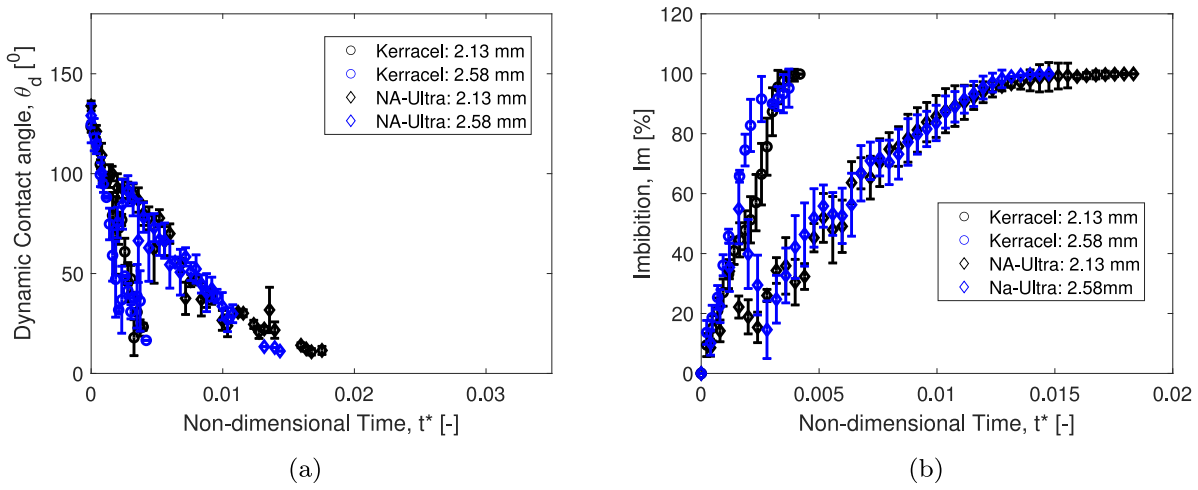

Fig. 13. Effect of exudate volume on (a) Dynamic contact angle (b) Imbibition.

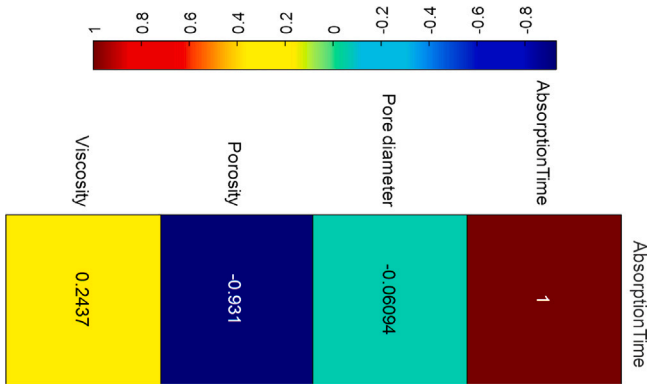

Fig. 14. Correlation matrix heatmap between absorption time and various factors.

correlation coefficient of −0.931 between porosity and absorption time is notably strong and negative. This indicates that higher porosity is linked to shorter absorption times, meaning that materials with greater porosity absorb liquids more rapidly. Supporting this, Choi et al. (2017) observed an increase in penetration depth with increasing porosity [34].

In contrast, the correlation coefficient for pore diameter is −0.06094, suggesting that the size of individual pores has minimal effect on the rate of absorption. This result implies that the influence of pore diameter on absorption is negligible compared to other factors, such as porosity. The stronger effect of porosity indicates that the overall volume of void spaces (i.e., porosity) within a material is a more crucial factor in determining the rate of liquid absorption than the size of individual pores. This is likely because porosity affects the total space available for liquid absorption, whereas pore diameter alone does not significantly impact the ease of liquid entry into the material.

Additionally, the moderate positive correlation between viscosity and absorption time reveals that as the viscosity of the liquid increases, the absorption time also lengthens. This finding aligns with observations by [15,35], and is intuitive because more viscous liquids flow more slowly and therefore take longer to penetrate porous materials.

These correlation coefficients provide insights into whether changes in one variable are associated with changes in another variable and the strength and direction of that association, which will help in developing better wound dressings and, hence, better wound management. For instance, if rapid absorption is desired, focusing on increasing porosity might be more beneficial than altering pore diameter. Additionally, for fluids with varying viscosities, adjustments might be needed to account for the resulting changes in absorption times.

4. A note on the clinical implications

The results of this study have profound implications for clinical wound care management. The detailed quantitative analysis of wound exudate absorption by different dressings provides practical guidance for clinicians. For faster absorption of moderate to heavy exudate, Kerracel is the preferred choice due to its superior absorption rate. Between NA Ultra and Atrauman, both of which are used as primary dressings in conjunction with a secondary dressing, NA Ultra will be the preferred choice as it absorbs more exudate compared to Atrauman.

Clinicians should select wound dressings tailored to specific wound characteristics and patient conditions, such as high-viscosity exudates or patients with high blood sugar levels. High-viscosity exudates and hyperglycemia conditions slow down absorption, making a personalized approach crucial to enhancing healing rates and reducing complications. For such cases, natural-based and high-porosity materials should be considered for faster absorption of the wound exudate.

For large volumes of exudate, dressings with larger porosity and pore diameter are essential for faster and more efficient absorption. This approach may improve patient comfort, reduce the risk of infection, and accelerate the healing process, particularly for chronic wounds that are slow to heal.

5. Conclusion

The study investigates how wound exudate interacts with wound dressings to enhance wound management by better understanding the complex dynamics of exudate absorption using high spatial and temporal resolution imaging. Seven commercially available wound dressings were used in the present study, categorized based on clinical and material perspectives into: polyester-based (Kerramax and Melolin), natural-based (Aquacel, Kerracel, and Kaltostat), and knitted (Atrauman and NA Ultra). Three different working fluids were used to investigate various scenarios of exudate interaction with the dressings—normal wound exudate (SBF), chronic wound exudate (SBF with Dextran Blue), and high blood sugar level exudate (SBF with glucose). Key findings include:

- NA Ultra has the highest fibre diameter and porosity, indicating a better probability of exudate absorption and moisture retention compared to other wound dressings.
- The present investigation reveals that absorption dynamics are significantly influenced by the physical and chemical properties of the dressing materials. Kerracel (made of natural cellulose) generally provides superior absorption quality due to its different physical and chemical properties.

- Two different droplet landing outcomes were observed — complete penetration and partial imbibition. Partial imbibition occurs only for Melolin and Atrauman, where the droplets get 'pinned' due to the hydrophobic nature of their surfaces. Complete penetration of droplets into the wound dressing material is due to the combined action of both hydrodynamic focusing and capillary forces. This combined mechanism enhances the overall effectiveness of the wound dressing in managing wound exudate.
- In the case of stand-alone dressings, cellulose-based dressings such as Kerracel and Aquacel absorb faster compared to alginate-based wound dressings (Kaltostat).
- With the increase in exudate volume and high blood sugar levels, the absorption time of the exudate in the wound dressing increases due to the increased viscosity and reduced surface tension of the exudates.
- From the correlation matrix, it was observed that porosity has a more significant effect on the absorption time, followed by viscosity.

These insights provide a robust foundation for improving clinical practices in wound care, guiding the development of advanced dressings, and enhancing patient care outcomes. In a parallel study carried out under the same project, it was observed that some of the cattle exudates are shear-thinning fluids [9]. Thus, future work will involve conducting experiments using shear-thinning fluids and investigating flow inside a thin layer of the wound dressings using a μ-PIV system.

CRediT authorship contribution statement

Avick Sinha: Writing – review & editing, Writing – original draft, Validation, Software, Methodology, Investigation, Formal analysis, Data curation, Conceptualization. **Anastasios Georgoulas:** Writing – review & editing, Supervision, Project administration, Funding acquisition, Conceptualization. **Cyril Crua:** Writing – review & editing, Supervision, Project administration, Investigation, Conceptualization. **Shirin Saberianpour:** Writing – review & editing. **Dipak Sarker:** Writing – review & editing. **Rachel Forss:** Writing – review & editing. **Matteo Santin:** Writing – review & editing, Supervision, Project administration, Investigation, Funding acquisition.

Declaration of competing interest

The authors declare the following financial interests/personal relationships which may be considered as potential competing interests: Matteo Santin reports financial support was provided by University of Brighton. Matteo Santin reports a relationship with University of Brighton that includes: funding grants and travel reimbursement. If there are other authors, they declare that they have no known competing financial interests or personal relationships that could have appeared to influence the work reported in this paper.

Acknowledgements

This work is supported by the UKRI Engineering and Physical Science Research Council, grant number EP/W023164/1.

Appendix A. Supplementary data

Supplementary material related to this article can be found online at https://doi.org/10.1016/j.expthermflusci.2025.111408.

Data availability

Data will be made available on request.

References

[1] L. Atkin, Z. Bućko, E.C. Montero, K. Cutting, C. Moffatt, A. Probst, W. Tettelbach, Implementing TIMERS: the race against hard-to-heal wounds, J. Wound Care 28 (2019) S1–S50.
[2] B. Kyaw, K. Jaerbrink, L. Martinengo, J. Car, K. Harding, A. Schmidtchen, Need for improved definition of chronic wounds in clinical studies, Acta Dermato-Venereologica 98 (1) (2017) 157–158.
[3] L. Martinengo, M. Olsson, R. Bajpai, M. Soljak, Z. Upton, A. Schmidtchen, J. Car, K. Järbrink, Prevalence of chronic wounds in the general population: systematic review and meta-analysis of observational studies, Ann. Epidemiol. 29 (2019) 8–15.
[4] O.Q. Goh, G. Ganesan, N. Graves, Y.Z. Ng, K. Harding, K.B. Tan, Incidence of chronic wounds in Singapore, a multiethnic Asian country, between 2000 and 2017: a retrospective cohort study using a nationwide claims database, BMJ Open 10 (9) (2020).
[5] H. Derakhshandeh, S.S. Kashaf, F. Aghabaglou, I.O. Ghanavati, A. Tamayol, Smart bandages: the future of wound care, Trends Biotechnol. 36 (12) (2018) 1259–1274.
[6] G. FrykbergRobert, et al., Challenges in the treatment of chronic wounds, 2015.
[7] M. Andredaki, A. Georgoulas, M. Marengo, Numerical investigation of quasi-sessile droplet absorption into wound dressing capillaries, Phys. Fluids 32 (9) (2020).
[8] C. Dowsett, Exudate management: a patient-centred approach, J. Wound Care 17 (6) (2008) 249–252.
[9] G. Melotto, A. Sinha, J.R. Forss, Exploring exudate viscosity: A rheological analysis of wound exudates, Wound Repair Regen. (2024).
[10] S. Saberianpour, G.Melotto, R. Forss, L. Redhead, J. Elsom, N. Terrazzini, S. Sandeman, D. Sarker, G. Bucca, A. Hesketh, et al., Development of theranostic wound dressings: harnessing the knowledge of biospecific interactions at the biomaterial interface to promote healing and identify biomarkers, Expert. Rev. Med. Devices 20 (3) (2023) 163–165.
[11] S. Dhivya, V.V. Padma, E. Santhini, Wound dressings–a review, BioMedicine 5 (4) (2015) 22.
[12] Y. Suzuki, M. Tanihara, Y. Nishimura, K. Suzuki, Y. Yamawaki, H. Kudo, Y. Kakimaru, Y. Shimizu, In vivo evaluation of a novel alginate dressing, J. Biomed. Mater. Res. 48 (4) (1999) 522–527.
[13] K.W. Ng, H.N. Achuth, S. Moochhala, T.C. Lim, D.W. Hutmacher, In vivo evaluation of an ultra-thin polycaprolactone film as a wound dressing, J. Biomater. Sci. Polym. Ed. 18 (7) (2007) 925–938.
[14] S. Saberianpour, G. Melotto, L. Redhead, N. Terrazzini, J.R. Forss, M. Santin, Harnessing the interactions of wound exudate cells with dressings biomaterials for the control and prognosis of healing pathways, Pharmaceutic.
[15] J.R. Forss, Does exudate viscosity affect its rate of absorption into wound dressings? J. Wound Care 31 (3) (2022) 236–242.
[16] N.H.M. Nguyen, T.T.N. Le, A.T. Nguyen, H.N.T. Le, T.T. Pham, Biomedical materials for wound dressing: Recent advances and applications, RSC Adv. 13 (8) (2023) 5509–5528.
[17] A.L. Yarin, Drop impact dynamics: Splashing, spreading, receding, bouncing..., Annu. Rev. Fluid Mech. (38) (2006) 159–192.
[18] S.A. Sinha, V. Ramakrishnan, K. Johnson, Droplet impact on a curved moving liquid film, in: Turbo Expo: Power for Land, Sea, and Air, 86106, American Society of Mechanical Engineers, 2022, p. 19, V10BT31A003, 2022.
[19] M. Weclas, Potential of porous-media combustion technology as applied to internal combustion engines, J. Thermodyn. (2010).
[20] W.S. Kim, S.Y. Lee, Behavior of a water drop impinging on heated porous surfaces, Exp. Therm Fluid Sci. (55) (2014) 62–70.
[21] K. Wallace, K. Yoshida, Determination of dynamic spread factor of water droplets impacting on water-sensitive paper surfaces, J. Colloid Interface Sci. 63 (1) (1978) 164–165.
[22] V. Starov, S. Zhdanov, S. Kosvintsev, V. Sobolev, M. Velarde, Spreading of liquid drops over porous substrates, Adv. Colloid Interface Sci. 104 (1–3) (2003) 123–158.
[23] A. Delbos, E. Lorenceau, O. Pitois, Forced impregnation of a capillary tube with drop impact, J. Colloid Interface Sci. 341 (1) (2010) 171–177.
[24] D. Bouchard, M. Andredaki, A. Georgoulas, M. Marengo, S. Chandra, Penetration characteristics of a liquid droplet impacting on a narrow gap: Experimental and numerical analysis, Phys. Fluids 34 (5) (2022).
[25] R. Sahu, S. Sett, A. Yarin, B. Pourdeyhimi, Impact of aqueous suspension drops onto non-wettable porous membranes: Hydrodynamic focusing and penetration of nanoparticles, Colloids Surf. A (467) (2015) 31–45.
[26] C. Boscariol, S. Chandra, D. Sarker, C. Crua, M. Marengo, Drop impact onto attached metallic meshes: liquid penetration and spreading, Exp. Fluids (59) (2018) 1–13.
[27] J. Lee, D. Derome, J. Carmeliet, Drop impact on natural porous stones, Phys. Rev. Lett. 118 (1) (2016).
[28] S. Ryu, P. Sen, Y. Nam, C. Lee, Water penetration through a superhydrophobic mesh during a drop impact, APS, unknown edition edition, 2017.
[29] N. Lipson, S. Chandra, Cooling of porous metal surfaces by droplet impact, Int. J. Heat Mass Transfer (152) (2020) 119494.

[30] T.C. de Goede, A.M. Moqaddam, K. Limpens, S. Kooij, D. Derome, J. Carmeliet, N. Shahidzadeh, D. Bonn, Droplet impact of Newtonian fluids and blood on simple fabrics: Effect of fabric pore size and underlying substrate, Phys. Fluids 33 (3) (2021).
[31] G. Zhang, M.A. Quetzeri-Santiago, C.A. Stone, L. Botto, J.R. Castrejón-Pita, Droplet impact dynamics on textiles, Soft Matter 14 (40) (2018) 8182–8190.
[32] N.C. Reis Jr., R.F. Griffiths, J.M. Santos, Numerical simulation of the impact of liquid droplets on porous surfaces, J. Comput. Phys. 198 (2) (2004) 747–770.
[33] H.K. Navaz, B. Markicevic, A.R. Zand, Y. Sikorski, E. Chan, 2.M. Sanders, T.G. D'Onofrio, Sessile droplet spread into porous substrates—Determination of capillary pressure using a continuum approach, J. Colloid Interface Sci. 325 (2) (2008) 440–446.
[34] M. Choi, G. Son, W. Shim, Numerical simulation of droplet impact and evaporation on a porous surface, Int. Commun. Heat Mass Transfer (80) (2017) 18–29.
[35] A. Basit, K. KuShaari, P. Siwayanan, B. Azeem, Effect of process parameters on droplet spreading behaviour over porous surface, Can. J. Chem. Eng. 96 (1) (2018) 352–359.
[36] F. Baino, S. Yamaguchi, The use of simulated body fluid (SBF) for assessing materials bioactivity in the context of tissue engineering: review and challenges, Biomimetics 5 (4) (2020) 57.
[37] M. ietrzyńska, A. Voelkel, Stability of simulated body fluids such as blood plasma, artificial urine and artificial saliva, Microchem. J. (134) (2017) 197–201.
[38] N.N. Wahab, E.A. Cowden, N.J. Pearce, M.J. Gardner, H. Merry, J.L. Cox, Is blood glucose an independent predictor of mortality in acute myocardial infarction in the thrombolytic era? J. Am. Coll. Cardiol. 40 (10) (2002) 1748–1754.
[39] A.J. Boulton, D.G. Armstrong, R.S. Kirsner, C.E. Attinger, L.A. Lavery, B.A. Lipsky, J.L. Mills Sr, J.S. Steinberg, Diagnosis and Management of Diabetic Foot Complications, Am Diabetes Assoc, 2018.
[40] R.A. Rabbani, S. Salehi, Dynamic modeling of the formation damage and mud cake deposition using filtration theories coupled with SEM image processing, J. Nat. Gas Sci. Eng. (42) (2017).
[41] B.S. Barnett, S. Irving, Studies of wound healing and the effects of dressings, high performance biomaterials, Routledge (2017) 583–620.
[42] J. Stephen-Haynes, The use of Atrauman®non-adherent wound dressing in tissue viability, Br. J. Community Nurs. 14 (Sup1) (2009) S29–S34.
[43] J. Jones, J. Barraud, An evaluation of KerraMax care in the management of moderate to heavily exuding wounds, Br. J. Community Nurs. 19 (Sup3) (2014) S48–S53.
[44] Y. Barnea, J. Weiss, E. Gur, A review of the applications of the hydrofiber dressing with silver (Aquacel Ag®) in wound care, Ther. Clin. Risk Manag. (2010) 21–27.
[45] N. Jones, N. Ivins, V. Ebdon, S. Hagelstein, K. Harding, A case series evaluating the use of a gelling fibre dressing for moderate to highly exuding wounds, Wounds UK 13 (3) (2017).
[46] F. Burton, An evaluation of non-adherent wound-contact layers for acute traumatic and surgical wounds, J. Wound Care 13 (9) (2004) 371–373.
[47] C.-T. Chiu, J.-S. Lee, C.-S. Chu, Y.-P. Chang, Y.-J. Wang, Development of two alginate-based wound dressings, J. Mater. Sci., Mater. Med. (19) (2008).
[48] G. Birkhoff, D.P. MacDougall, E.M. Pugh, S.G. Taylor, Explosives with lined cavities, J. Appl. Phys. 19 (6) (1948) 563–582.
[49] D.A. Weiss, A.L. Yarin, Single drop impact onto liquid films: neck distortion, jetting, tiny bubble entrainment, and crown formation, J. Fluid Mech. (385) (1999) 229–254.
[50] S. Thoroddsen, The ejecta sheet generated by the impact of a drop, J. Fluid Mech. (451) (2002) 373–381.
[51] E.-E. Tudoroiu, C.-E. inu Pîrvu, M.G. Albu Kaya, L. Popa, V. Anuta, R.M. Prisada, M.V. Ghica, An overview of cellulose derivatives-based dressings for wound-healing management, Pharmaceuticals 14 (12) (2021).
[52] R. Abka-Khajouei, L. Tounsi, N. Shahabi, A.K. Patel, S. Abdelkafi, P. Michaud, Structures, properties and applications of alginates, Mar. Drugs 20 (6) (2022) 364.
[53] S. Hampton, A. Coulborn, M. Tadej, C. Bree-Aslan, Using a superabsorbent dressing and antimicrobial for a venous ulcer, Br. J. Nurs. 20 (Sup8) (2011) S38–S43.
[54] M. Uzun, S. Anand, T. Shah, In vitro characterisation and evaluation of different types of wound dressing materials, J. Biomed. Eng. Technol. (1) (2013) 1–7.
[55] K. Vontas, C. Boscariol, M. Andredaki, A. Georgoulas, C. Crua, J.H. Walther, M. Marengo, Droplet impact on suspended metallic meshes: Effects of wettability, reynolds and weber numbers, Fluids 5 (2) (2020) 81.
[56] P. Sedgwick, Pearson's correlation coefficient, Br. Med. J. Publ. Group (345) (2012).